

# Voyager LECP

## Introduction

### 1.0 LECP Instrument Summary

#### 2.0 LEPT System

- 2.1 Analog Processing
- 2.2 Species Separation
- 2.3 Pulse Height Discriminators
- 2.4 Timing and Rate Logic
- 2.5 Anticoincidence Shield
- 2.6 Special Features of D1 Subchannel
- 2.7 Pulse Height Analyzer

#### 3.0 LEMPA System

- 3.1 Alpha Channel
- 3.2 Beta and Gamma Channels
- 3.3 Beta Prime
- 3.4 A,B Channels
- 3.5 Delta, Delta Prime Channels

#### 4.0 Hybrid Circuits

- 4.1 Linear Amplifier (0247)
- 4.2 Logarithmic Amplifier (0254)
- 4.3 LEPT Discriminator (0262)
- 4.4 Dual One Shot (0263)
- 4.5 Fast Amplifier and Discriminator (0257 and 0277)

#### 5.0 Commands, Operating Modes and Formats

- 5.1 Command Structure
- 5.2 Operating Modes
- 5.3 Status Words
- 5.4 Scanning System
- 5.5 In Flight Calibrator

In late summer of 1977 the Voyager 1 and Voyager 2 spacecraft were launched from Cape Canaveral, beginning a tour of the outer solar system that would include encounters with the planetary systems of Jupiter, Saturn, Uranus and Neptune. Among the science payloads carried aboard these spacecraft were the Low Energy Charged Particle (LECP) instruments, designed and built by the Applied Physics Laboratory with the help of co-investigator institutions including the University of Maryland, the University of Kansas and Bell Laboratories. The LECP was the first of many APL instruments to be flown on a planetary probe.

The LECP was designed to perform pioneering measurements of the energetic particle environments in the vicinity of Saturn and Uranus, and to perform second generation studies (following the earlier results obtained from Pioneer 10 and 11) of the charged particle population trapped in the Jovian magnetosphere. In addition, the LECP design included the capability to carry out comprehensive spectral, composition and anisotropy measurements in the interplanetary medium on radiation of solar and galactic origin. General features and science objectives of the LECP have been described by *Krimigis et al, 1977*.

Data obtained from these instruments have been extensively analyzed for some twenty years now and the results discussed and published widely. Additional data, from the vicinity of the heliopause and beyond, are still being received and studied. The present document summarizes the main engineering features of the LECP electronics, in order to shed some light on the design ideas that went into it and the means by which these ideas were implemented. The reader might bear in mind that this instrument was designed in the early to mid 1970's. No microprocessors had yet been flown, printed circuit boards were still laid out by hand, 4000-series CMOS was the most advanced digital logic family commercially available, and the analog-to-digital converter was a slow and cumbersome system requiring boards full of discrete components. Nevertheless some aspects of the LECP design, particularly in the acquisition and front-end processing of the raw detector signals, have proven resilient over the years and modern implementations on recent space missions have changed remarkably little to the present day.

## **1.0 LECP Instrument Summary**

The LECP consists of two essentially independent systems, viz. the Low Energy Particle Telescope (LEPT) and the Low Energy Magnetospheric Particle Analyzer (LEMPA). Each of these was designed to operate during particular phases of the mission; they are described in some detail in Sections 2 and 3 of this document. For the long periods spent in interplanetary space the instrument is operated in Cruise Mode, during which the LEPT system is fully active, as is part of the LEMPA system. During part of the Jovian encounter, the LEPT was switched off and the remaining portions of the LEMPA system were activated. Overall power consumption is 4.2 watts in either operating mode.

Instrument weight is 7.4 kilograms. Both sensor telescopes are mounted on a rotating platform whose motion is controlled by a stepping motor operated from the spacecraft Flight Data System (FDS). This allowed the sensors to scan 360 degrees, over eight equally spaced sectors, in the ecliptic plane. Because of the need to closely couple the front-end electronics to the detectors, these circuit assemblies were likewise mounted on the rotating platform. The remainder of the electronic systems was packaged in the

fixed, or lower, section of the LECP, thereby minimizing the load requirements on the motorized assembly. The overall instrument is depicted in Figure 1.1.

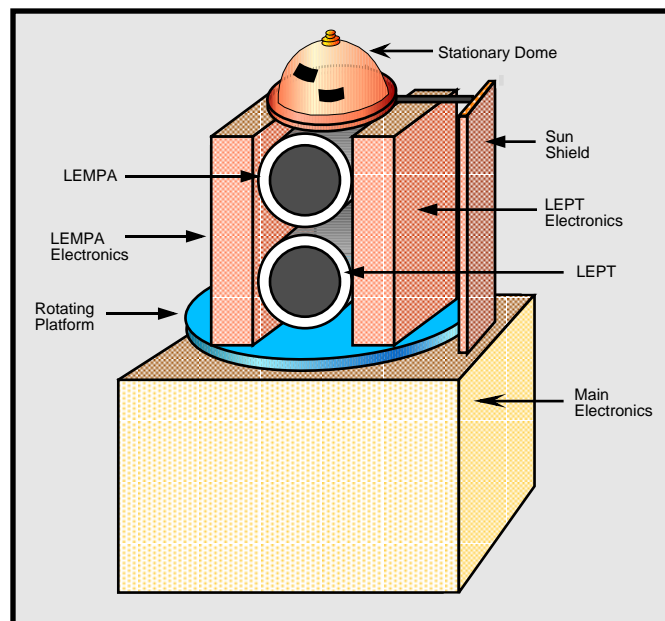


Figure 1.1 LECP Instrument

Electrical interfaces between the upper and lower sections were carried on a multi-conductor flexible printed circuit assembly known as the "polytwist" whose upper end rotated with the stepping platform. As a result the motor rotation was limited to one revolution in either direction. During Cruise Mode the stepping rate was one revolution every 48 minutes, later revised to 25.6 minutes. For the planetary encounters the rotation period was shortened to 3.2 minutes, while a special operating mode at perijove allowed a complete revolution every 1.6 minutes. A sun shield at the 0-degree position allowed the telescopes to be "stowed" indefinitely. This feature prevented direct sunlight from striking the exposed detectors in both telescopes during the early phase of the mission, and also allowed background measurements to be performed during the planetary encounters. Additionally, weak radioactive sources mounted on the inside surface of the sun shield provided a means of inflight calibration for both telescope systems.

One of the keys in the design and building of the LECP was the development of a family of hybrid microcircuits which were used extensively as standardized modules throughout the instrument electronics. Limitations on instrument mass and size prohibited the use of discrete components for most of the required functions. Moreover, there were at the time no commercially available integrated circuits that could perform these functions at reasonable power consumption while yielding the necessary speed and precision. Compounding these problems was the question of radiation hardness required to survive the intense environment anticipated in the Jovian encounter. The use of specially designed hybrid modules addressed these problems, while allowing the bulk of the electronic circuitry to be tested for performance and reliability prior to board level assembly. In all, there were twelve different hybrid designs used in the LECP instrument, totaling some 260 modules. Some of these, most notably the 0247 general purpose linear amplifier and the 0254 logarithmic converter, were carried over essentially unchanged

into the next generation of APL instruments, continuing to operate to the present day on five different interplanetary spacecraft.

## 2.0 LEPT System

The Low Energy Particle Telescope (LEPT) is a bi-directional dE vs E sensor, illustrated in Figure 2.1. It consists of five axially spaced elements, D1 through D5, of which the front element D1 is a coplanar set of three very thin detectors designated D1A, D1B, and D1C. This main array is surrounded by an active anticoincidence shield consisting of eight identical large area detectors arranged in a cylinder of octagonal cross-section. The system analyzes a broad spectrum of particles extending from protons through heavy nuclei, with energy coverage from 0.35 to approximately 1000 Mev/nucleon. All events processed by the LEPT are sorted into a set of Rate Channels corresponding to discrete groupings of energy and mass. Particular events, selected by a rotating priority system, are analyzed to eight bit precision in dE and E by the Pulse Height Analyzer. A block diagram of the LEPT system is given in Figure 2.2.

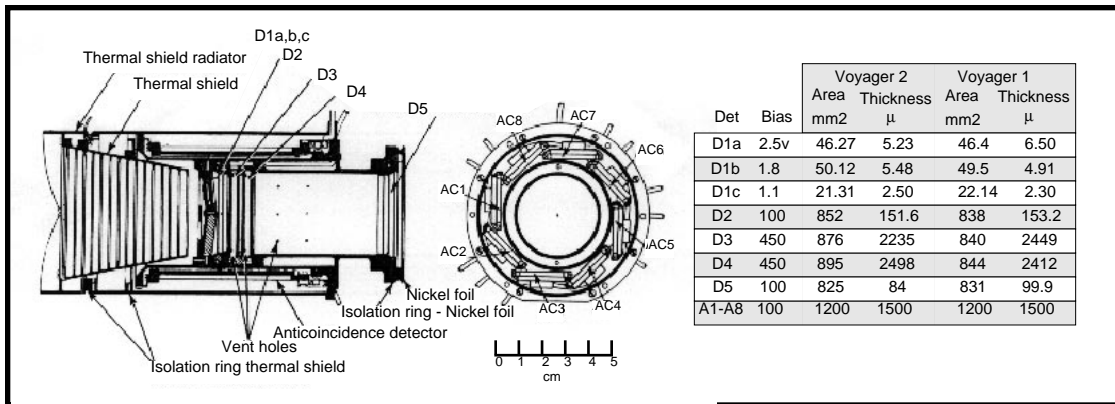


Figure 2.1 LEPT Sensor Assembly

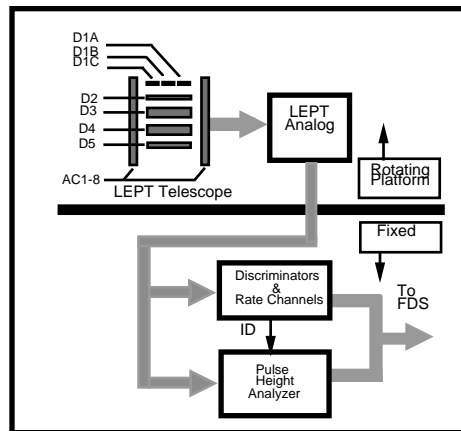


Figure 2.2 Block Diagram, LEPT

The circuitry for the D1-D5 detector signals follows a common pattern, implemented by use of a set of standardized hybrid modules designed specifically for the LEPT system. In each channel the detector output is collected by a charge sensitive preamplifier, filtered and shaped by a pair of cascaded linear stages, range compressed by a logarithmic amplifier and buffered by an output linear stage. Despite the wide variations in detector thicknesses and the associated differences in dynamic range and noise, the processing channels are essentially similar both schematically and in layout, differing for the most part only in component values. Processing of the anticoincidence

signals follows the same pattern again, with the exception that no logarithmic conversion is performed. In the case of the D1 detectors the two stages of linear filtering are performed independently on the D1A, D1B and D1C signals; these are summed at the input to the D1 logarithmic amplifier.

The LEPT channels are individually power switched under LECP command. This feature provides a margin of reliability in that any failure of either a detector or electronic component can be isolated and that channel taken off line, thereby preserving a significant part of the LEPT capability. In addition, this switching feature afforded significant power saving during Jovian encounter, when the radiation flux rates were expected to exceed the capacity of the LEPT system in any case.

## 2.1 Analog Processing

The analog processing format for the LEPT detector signals is summarized in block format in Figure 2.3. The schematic diagram in Figure 2.4 illustrates in detail the design of the D2 channel, which for these purposes may be taken as representative of all the analog circuitry throughout the LEPT system. The complete analog channel depicted is laid out on a single daughterboard, mounted to the motherboard by means of soldered pin connections.

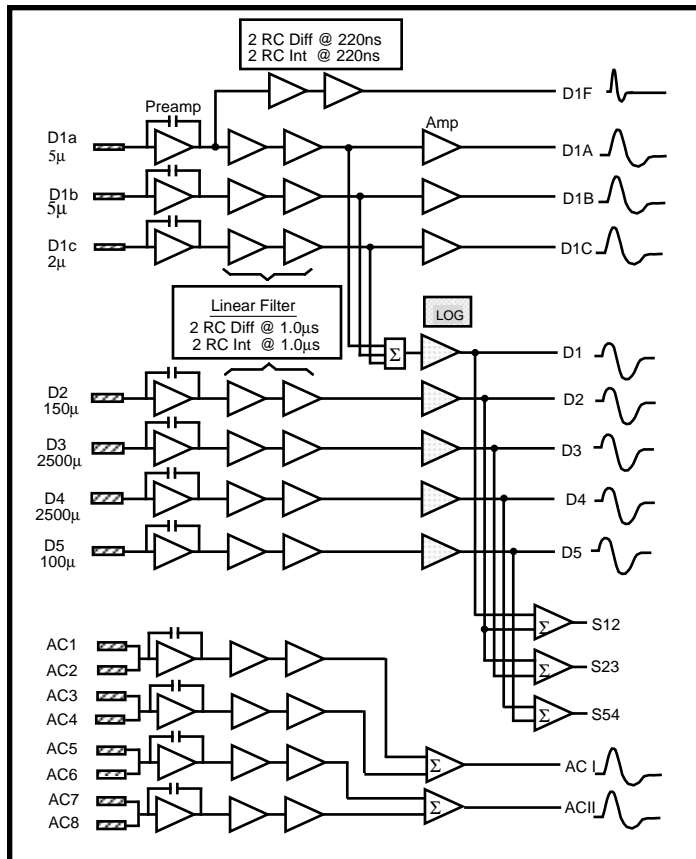


Figure 2.3 LEPT Analog Electronics

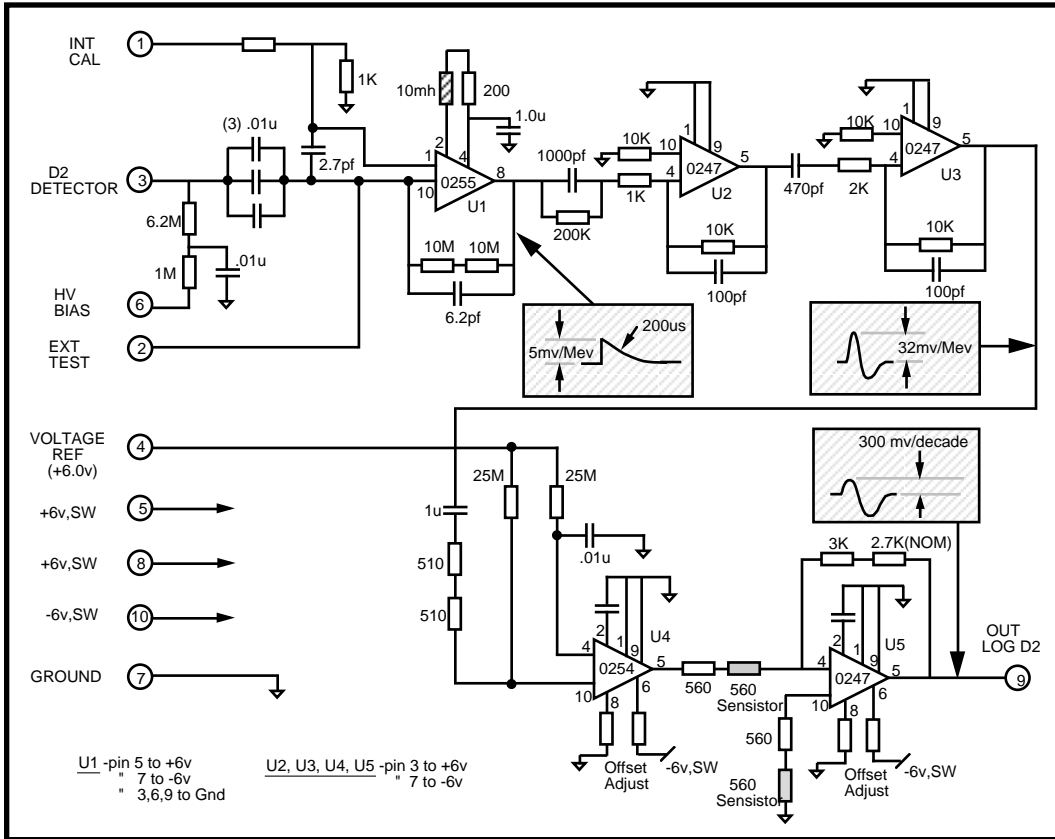


Figure 2.4 D2 Channel Schematic

The board contains five hybrid modules: a charge preamp U1, three linear amplifiers (U2,U3,U5) and a logarithmic amplifier U4. The feedback around the preamp is 6.2 pf connected externally, in addition to the nominal value of 2.2 pf internal to the module. The resulting charge conversion factor is 5 mv/Mev when the effects of stray capacitance are included, with a decay time constant of 200  $\mu$ sec. Here the energy (in Mev) is the energy appearing as signal in the form of electron-hole pairs generated in the detector; it does not include energy lost in the dead layer or as pulse-height defect. Detector bias is brought in on board pin 6 and filtered by an R-C network. The detector connection is by means of miniature coaxial cable to pin 3. A parallel test input is provided at pin 2 for use in connecting a test generator, and the in-flight calibrate signal comes in at pin 1.

The connections to the linear amplifiers U2 and U3 each contain an RC high-pass network in the interstage coupling and an RC low-pass in the feedback. All four time constants are set to 1.0  $\mu$ s, yielding a characteristic bipolar step response with a zero-crossover at 3.0  $\mu$ s:

$$f(t) = [3 (t/\tau)^2 - (t/\tau)^3] e^{-t/\tau} , \tau=1.0 \mu s$$

The preamp decay time is compensated by a 200  $\mu$ s pole-zero cancellation network consisting of a 200K resistor operating in conjunction with the first 1000 pf coupling capacitor. For this D2 channel the peak signal amplitude at the output of the

second linear amp is 30 mv/Mev. This is fed through the 1K series resistance as a current mode signal into the logarithmic amp U4.

The log amp compares the input signal current to a reference current (200 na in the case of the D2 channel), yielding an inverted output pulse whose peak is proportional to the logarithm of the ratio between the peak signal current and the reference current according to the equations:

$$\frac{I_2}{I_1} = e^{\frac{q}{kT}(v_2 - v_1)}$$

$$\Delta V = \frac{kT}{q} \ln \frac{I_s + I_{ref}}{I_{ref}}$$

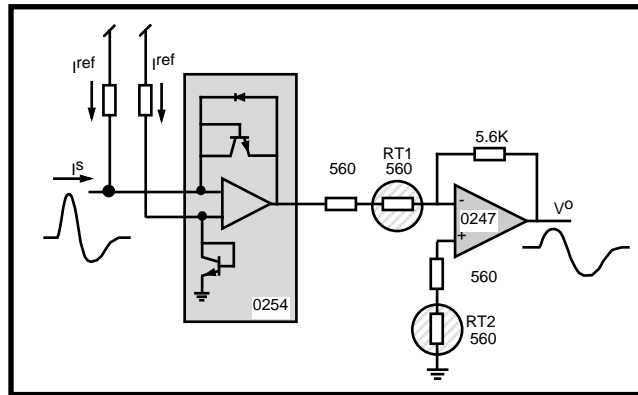


Figure 2.5 Log Amp Configuration

This pulse is then buffered and re-inverted by the linear stage U5, with a x5 gain. The arrangement is shown in Figure 2.5. The output stage also provides first order temperature compensation against the inherent temperature sensitivity of the log amp. This compensation is effected by the temperature-variable resistor (sensistor) RT1 in the input coupling, which varies the amplifier closed loop gain in opposition to the variation in the log amp output. The matching sensistor RT2 maintains the dc offset of U5 as RT1 changes.

Stability of dc offset is of critical importance in the LEPT overall design. Because of the asymmetry in the areas of the primary and secondary lobes caused by the characteristic nonlinearity of the logarithmic amplifier, all coupling to subsequent stages must be direct. For this reason both the log amp and linear amp hybrids were specifically designed for close dc tolerances. Moreover, the circuit board layouts contain provision for *in situ* trimming of residual offsets.



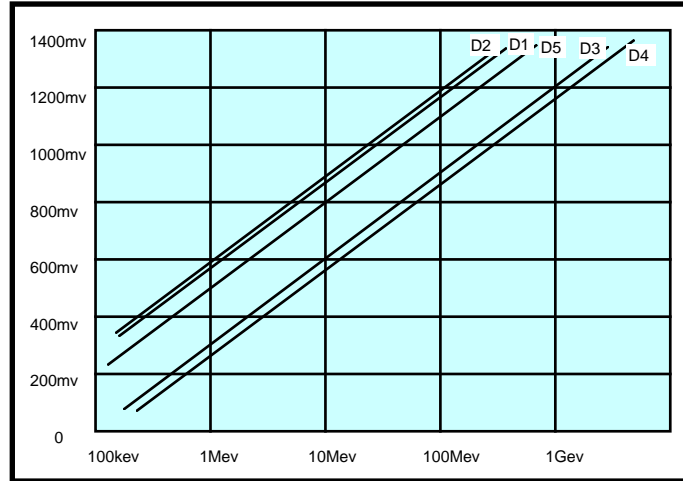


Figure 2.6 LEPT Log Response

The resulting output/input characteristics are plotted in Figure 2.6 above. These curves are unique for each of the channels according to the dynamic ranges required, and they are set by selection of preamp feedback capacitance, linear stage gain, and log reference current. The limiting factor in setting the minimum discrimination thresholds is channel noise. The most severe constraint is in the D1 channel because of the high capacitance (600-1200pf) associated with the thin detectors. In the D3 and D4 channels, the capacitance is relatively low, but the presence of 450v detector bias requires special breakdown protection networks at the preamp inputs; these networks are dominant noise sources in these channels. The nominal minimum threshold in the D1 channel is 300 Kev, or about three times the FWHM noise level arising from the parallel combination of the D1A, D1B and D1C subchannels. A special mode permits the D1B and D1C subchannels to be switched off. This reduces the overall noise level and allows the lowest D1 discriminator to operate at 200 Kev threshold, thereby extending the low energy limit of proton coverage.

## 2.2 Species Separation

For a two detector system in which a particle penetrates the first element (depositing energy  $dE$ ) and is stopped in the second (giving up the residual energy  $E$ ), points on a plot of  $dE$  vs  $E$  fall on unique tracks separated in atomic number and mass. Moreover, when plotted in log-log space, these tracks tend to follow relatively constant slopes over wide ranges of energy and mass. This allows species determination, as well as total energy measurement, by forming an appropriately weighted product of the form  $E_1 E_2^n$ , where  $E_1$  and  $E_2$  are the measured energy signals in the two detectors and the exponent  $n$  is approximately 0.6. The use of logarithmic amplifiers in this system carries obvious advantages. In addition to scale compression leading to wide operating dynamic range, it reduces the otherwise formidable task of fast analog multiplication to a simple linear addition. Further, the weighting factor  $n$  can be implemented by choice of a single resistor in the coupling to one arm of the summing junction. The resulting summed log signal is then treated in the same manner as the log signals representing energy depositions in forming rate channel boundaries.

## 2.3 Pulse Height Discriminators

The buffered log signals are coupled directly into parallel banks of pulse height discriminators as illustrated in Figure 2.10. The discriminators were arranged on a set of five daughter boards of identical layout mounted on the pulse circuit assembly (PCA) motherboard in the fixed lower section of the LECP. The specific thresholds are given in Table 2-1, with separate columns listing the final measured values for each of the three LECP units that were built.

All LEPT rate logic channels were derived from these discriminators. The logic equations are given as Table 2-2. The graphical representations of these equations, together with nominal species tracks, are illustrated in Figures 2.7 - 2.9.

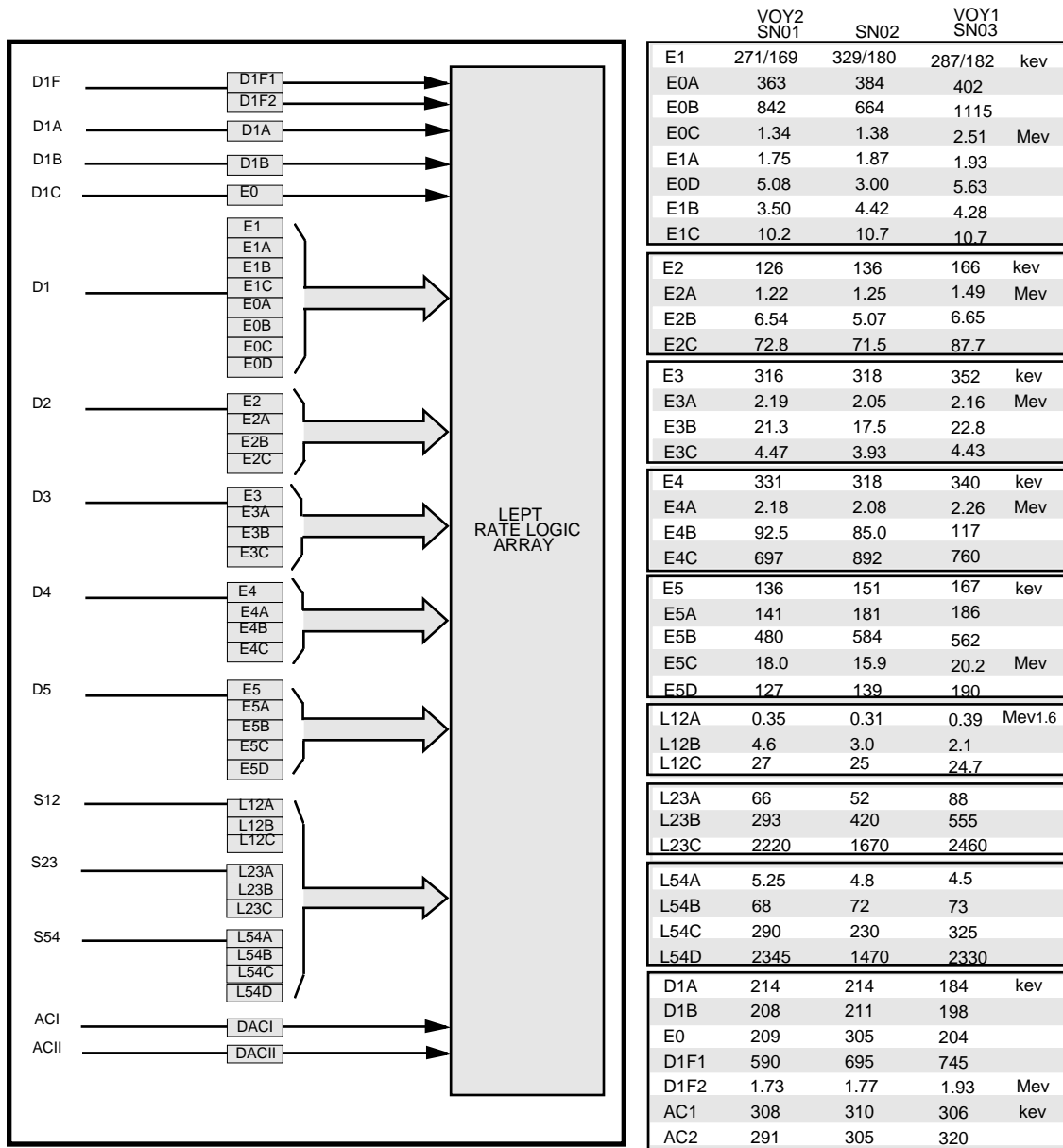


Figure 2.10 LEPT Discriminator Array

Table 2-1 LEPT Discriminator Settings

CH #	PASSBAND (MeV/nuc)		PRIORITY GROUP		CHANNEL LOGIC DEFINITION
	Voyager 1	Voyager 2			
1.	.57 - 1.78	.52 - 1.45	P	III	E1 (E1A) E2 (E2A) (E3) (L12A)
2.	1.2 - 2.7	1.2 - 2.7	P	III	E1 (E1A) E2A (E2B) (E3) (L12A)
3.	.46 - 1.80	.42 - 1.70	$\alpha$	III	E1 (E1A) E2A (E2B) (E3) L12A (L12B)
4.	1.9 - 4.0	1.8 - 4.0	$\alpha$	III	E1 (E1A) E2B (E3) L12A (L12B)
5.	0.6 - 4.2	0.6 - 4.2	L	II	E1 (E1B) E2 (E3) L12B (L12C)
6.	.53 - 5.6	.47 - 5.2	M	II	E1B (E1C) E2 (E2C) (E3)
7.	6.2 - 8.6	5.2 - 8.2	M	II	E1 (E1C) E2B L12C (E3)
8.	.31 - 2.2	.28 - 1.9	H	I	E1C E2 (E2C) (E3)
9.	2.3 - 12.0	2.0 - 12.0	H	I	E1B E2C (E3)
10.	4.4 - 9.2	4.4 - 11.4	P	III	E2A (E2B) E3 (E3B) (E4)
11.	9.2 - 21	11.4 - 20	P	III	E2 (E2A) E3A (E3B) (E4)
12.	4.2 - 7.8	4.2 - 7.8	$\alpha$	III	E2B (E2C) E3 (E4) (L23A)
13.	7.8 - 21	7.8 - 20	$\alpha$	III	E2 (E2B) E3B (E4) (L23A)
14.	5.5 - 33	5.5 - 33	L	II	E2A (E2C) E3 L23A (L23B) (E4)
15.	9.5 - 46	8.6 - 40	M	II	E2B E3A L23B (L23C) (E4)
43.	8.0 - 90	8.0 - 90	H	I	E2A E3A L23C (E4)
16.	3.4 - 17.6	3.0 - 17.3	P	III	E5B E4 (L54A) (E3)
17.	3.3 - 69	3.0 - 58	$\alpha$	III	E5B (E5C) E4 L54A (L54B) (E3)
18.	4.0 - 21	4.0 - 21	L	II	E5B (E5C) E4A L54B (L54C) (E3)
19.	6.8 - 10.4	6.0 - 9.2	M	II	E5C (E5D) E4 (E4B) L54C (L54D) (E3)
20.	10.4 - 40	9.6 - 42	M	II	E5B (E5D) E4B (E4C) L54C (L54D) (E3)
21.	9.5 - 18	8.2 - 17	H	I	E5B E4A (E4C) L54D (E3)
22.	19 - 78	18 - 82	H	I	E5B E4C L54D (E3)
23.	22 - 31	22 - 30	P	III	E5A (E5B) E4A (E4B) E3A (E2)
24.	22 - 31	22 - 30	$\alpha$	III	E5B (E5C) E4A (E4B) E3A (E2)
25.	48 - 64	44 - 61	M	II	E5B (E5C) E4B (E4C) E3B (E2)
26.	82 - 120	86 - 120	H	I	E5C E4B E3B (E2)
27.	34 - 71.5	37 - 89	P	III	E5A (E5B) E4A (E4B) E3A (E3B) E2 (E2A)
28.	33 - 62	31 - 56	$\alpha$	III	E5B (E5C) E4A (E4B) E3B E2 (E2B)
29.	68 - 270	69 - 270	M	II	E5B (E5C) E4B (E4C) E3B E2
30.	127 - 850	127 - 1000	H	I	E5C E4C E3B E2
31.	211 - 1000	213 - 1000	P	III	E4 (E4A) E3 (E3A)
32.	.28 - .69	.28 - .69	P	III	E0 (E0A) E2 (E2A) (E3)
33.	.20 - .51	.23 - .48	$\alpha$	III	E0A (E0B) E2 (E2A) (E3)
34.	.12 - .40	.12 - .40	L	II	E0B (E0C) E2 (E2A) (E3)
35.	.18 - .28	.20 - .34	M	II	E0C (E0D) E2 (E2A) (E3)
36.	.10 - .14	.10 - .14	H	I	E0D E2 (E2A) (E3)
37.	> 6	> 6	e <sup>-</sup>		E3C E4 (E2) (E5A) (E4A)
38.	.07 - .15	.06 - .20	L		E0B (E0D) (E2)
39.	.09 - .23	.10 - .20	$\alpha$		E0A (E0B) (E2)
40.					E5 E5A
41.					AL AR (Left & right shield coincidence)
42.					AL (Left) AR (Right) E0 E1 E2 E3 E4 E5
				Subcommutated	
44.	.35 - 1.5	.35 - 1.5	e <sup>-</sup>		E4 (E2) (E3) (E5A)
45.	> 2.5	> 2.5	e <sup>-</sup>		E4 E3A E2 (E5A) (E3C)
46.					D1F1
47.					D1F2

Table 2-2 LEPT Rate Channel Definitions

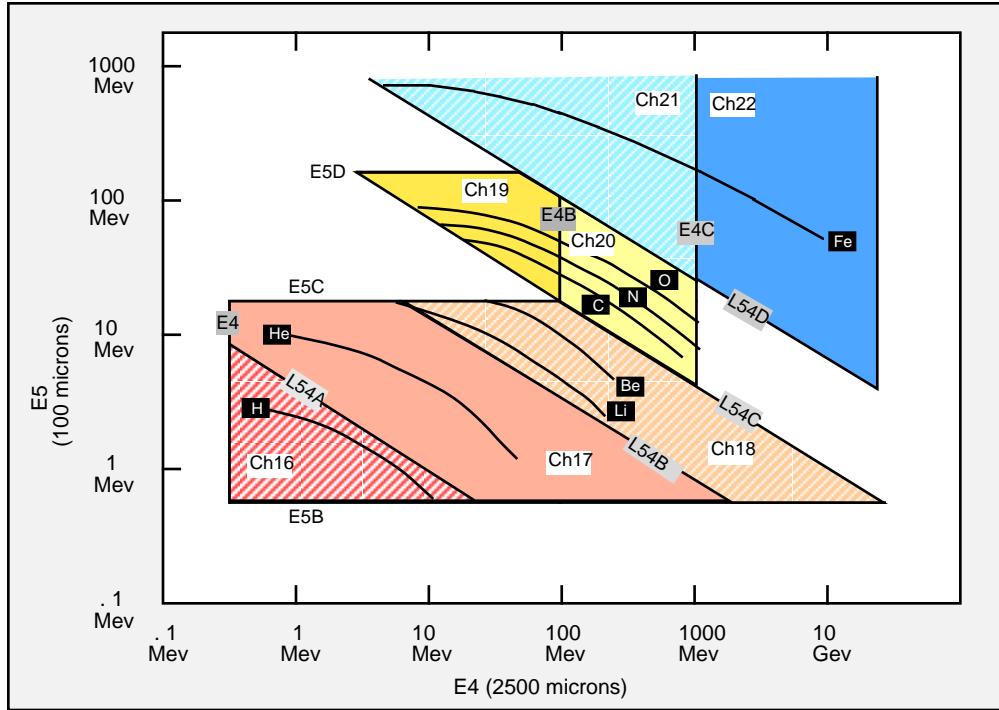


Figure 2.7  $\Delta E5$  vs  $E4$ , LEPT

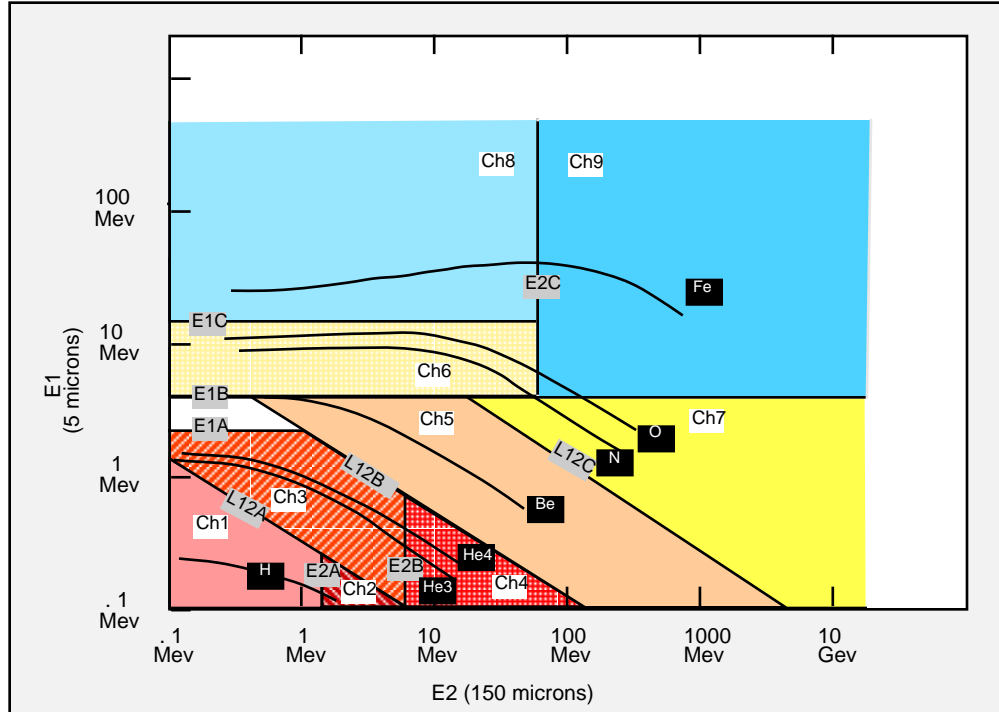


Figure 2.8  $\Delta E1$  vs  $E2$ , LEPT

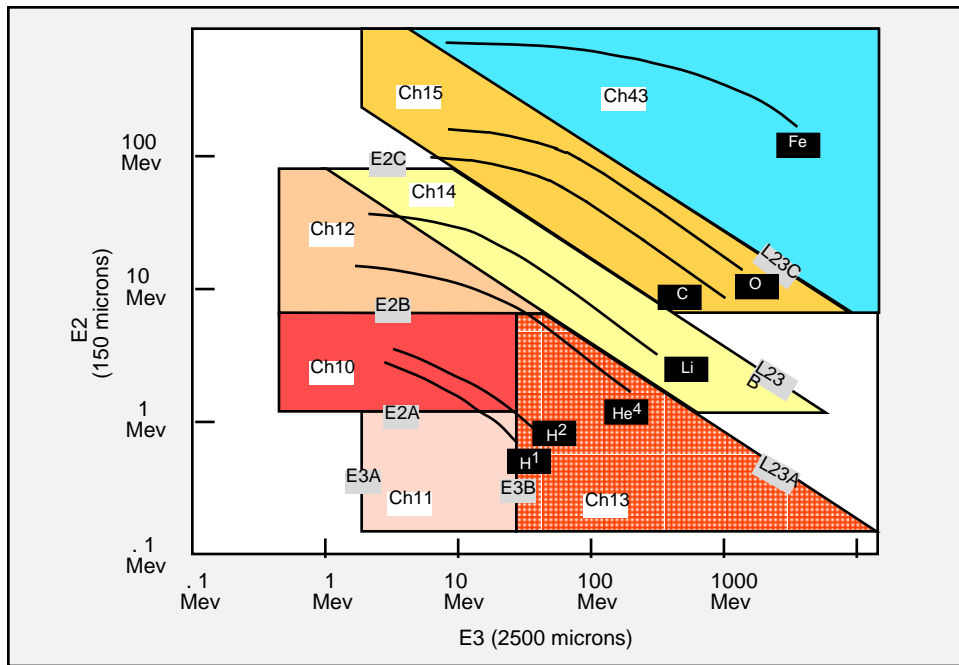


Figure 2.9  $\Delta E2$  vs  $E3$ , LEPT

## 2.4 Timing and Rate Logic

The leading edge of each discriminator output sets an R-S flip-flop, which stores the pulse throughout the timing and strobe sequence. This allows the rate channel logic to analyze the signals from all detectors corresponding to a given event. The storage flip-flops are located on two daughter boards in the PCA. They are returned to standby state at the end of each event by reset pulses generated in the timing circuitry, coming at a fixed time following the start of each event.

The timing sequence is initiated at the trailing edge of the output pulse from any of the lowest D1-D5 discriminators, corresponding to the zero crossover of the analog signal. The architecture and timing are illustrated in Figure 2.11. The trailing edge of the low level discriminator triggers a one-shot, generating a timing pulse of 1  $\mu$ s duration. These timing pulses, from each pair of adjacent detectors, are combined via logical AND operation, generating four 1  $\mu$ s strobe pulses designated S12, S23, S34 and S45. Each timing pulse trailing edge triggers a second one-shot to create a fixed 2.1  $\mu$ s delay, after which a third one-shot generates a 300 ns reset pulse to clear the R-S storage circuits and return the system to standby state.

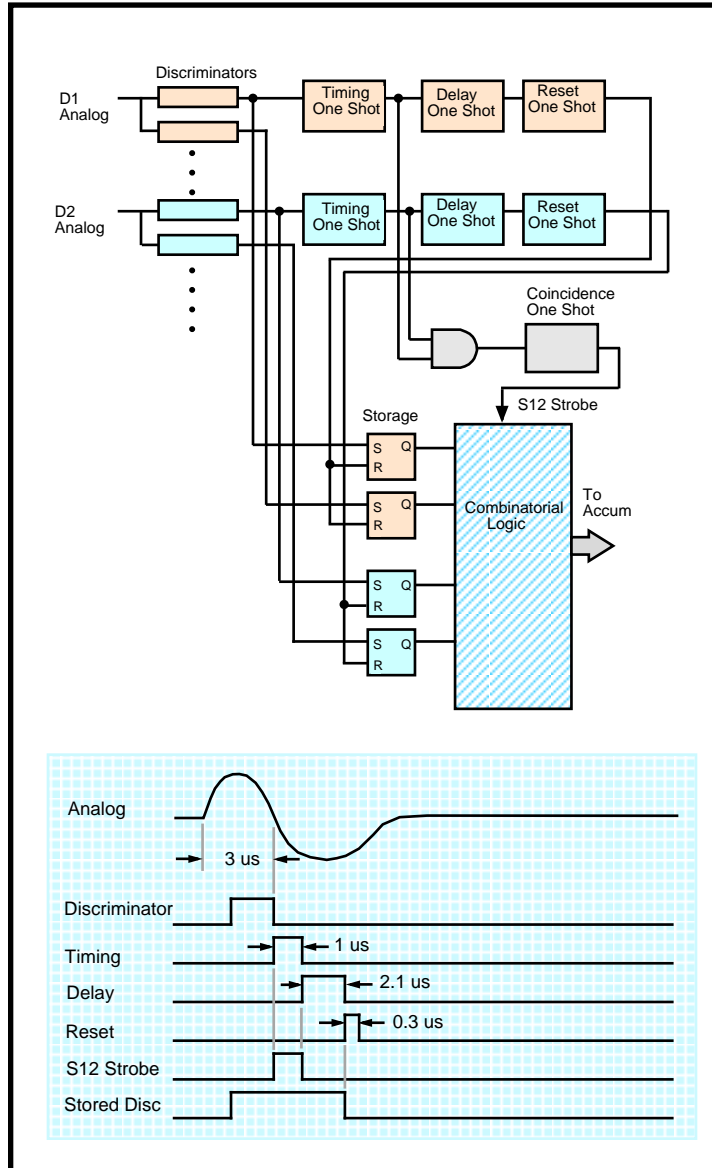


Figure 2.11 LEPT Rate Logic and Timing

The one-shots used for the timing, delay and reset functions are another hybrid design, packaged two to a module, with each consisting of an OTA and a CA4013 D-type flip-flop. Output pulse width is determined by an externally connected capacitor. The schematic and calibration curve are shown in Figure 4.5.

## 2.5 Anticoincidence Shield

The eight anticoincidence detectors are grouped into four pairs by direct parallel connection of adjacent detectors in the LEPT telescope assembly. Each of the resulting four signals connects to a charge sensitive preamplifier which drives a first filter-amplifier stage and a noninverting buffer containing the second differentiating network. Outputs from two such combinations are then further combined in a summing amplifier which also performs the second integration on the composite signal. Thus the detectors

AC1-4 provide a single analog output, designated ACI, representing the composite response of one continuous half of the cylindrical shield. The same scheme is used to combine the detectors AC5-8, forming the output ACII which corresponds to the second half of the shield. Filter time constants are  $1.0 \mu\text{s}$  as in the D1-D5 channels.

The ACI and ACII signals couple through the polytwist assembly into pulse height discriminators located on one of the PCA daughterboards. These discriminators are both set at 300 Kev. Their leading edges trigger one-shots which provide a blanking pulse to the rate channel logic array. The width of this pulse is  $9 \mu\text{s}$ , beginning at the discriminator leading edge, providing a minimum  $2.5\mu\text{s}$  margin before the onset of the coincidence strobe and a similar margin following the D1-D5 reset signals.

## 2.6 Special Features of the D1 Subchannel

The circuitry for the D1 detector includes three features unique within the LEPT system. First, the fact that D1 is actually a mosaic of three detectors requires that events in each of these be separately identified, since proper  $dE$  vs  $E$  analysis depends on knowledge of detector thickness. For this reason, separate pulse processing is performed through the second linear stage following each of the D1A, D1B and D1C charge preamps. The individual linear signals are detected by separate discriminators, each set lower than the first composite D1 threshold, taking advantage of the lower single detector noise levels. These discriminator outputs are stored in separate R-S flip-flops and included in the main logic array combinations under the normal strobe system. Reset of the R-S circuits is accomplished independently of the main system, following a delay of  $7.5\mu\text{s}$  generated from the discriminator leading edge.

Secondly, the D1A preamp is tapped off and coupled to a pair of linear filter stages with a  $220\text{ns}$  time constant. This allows clean operation at five times the maximum counting rate of the main channels and decreases primary pulse pile-up effects correspondingly. The fast linear signal drives two additional discriminators set at nominal levels of 600 Kev and 1.8 Mev. The set of analog waveforms characterizing the D1 subchannels are shown in Figure 2.12.

The third unique feature is the threshold selectability of the lowest composite D1 discriminator, allowing extension of LEPT coverage to low energy protons. Either the normal 300 Kev threshold or the special 200 Kev level can be chosen via LECP command. The lower value can be used when the D1B and D1C subchannels are commanded off. Under this condition, the overall noise level in the D1 channel is reduced to 60 Kev FWHM, arising solely from D1A. This feature was included for anticipated Far Encounter operations.

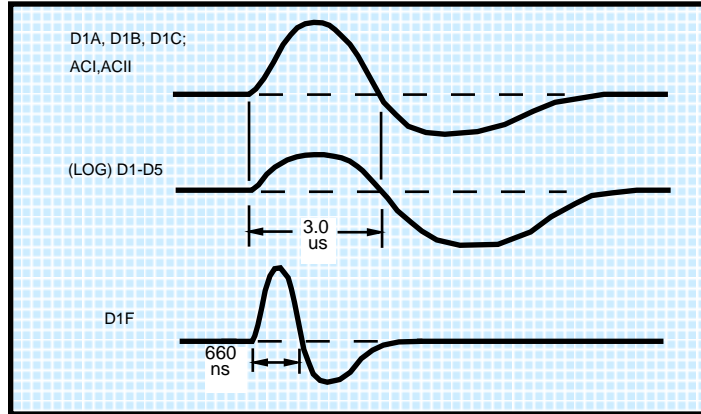


Figure 2.12 LEPT Analog Waveforms

## 2.7 Pulse Height Analyzer

The Pulse Height Analyzer (PHA) permits high precision measurements of selected events in the LEPT system. Whereas the rate channels analyze all events and assign them to discrete channels for accumulation and readout, the PHA provides fine determination of energy spectra for given species, as well as relative populations of different species within a larger group.

Because the PHA output consists of five eight-bit words per event, only a very limited sampling of events is actually analyzed and transmitted. This would be necessary even in the absence of telemetry limitations, since the PHA analysis cycle requires about one millisecond to complete. (Practical analog-to-digital converters, suitable for interplanetary spacecraft applications, were still several years away when the LECP was designed. The entire system, including peak-detect-and-hold circuits, control logic, multiplexers, successive approximation ADC, even the R-2R ladders, was synthesized from discrete components and occupied ten circuit boards in the LECP lower section.) The output for each event consists of one identifier word and four 8-bit words representing the amplitudes of the signals in each of four detectors. The ID word denotes the rate channel corresponding to the analyzed event. This word is defined in Table 2-3. Depending on the rate channel into which the event falls, either the D1 or D5 signal is analyzed, as are the D2, D3 and D4 signals. The analyzed events are read out in the LECP telemetry stream during cruise and far encounter modes of operation.

In order to allow measurement of energy and species distributions for the rarer species in the presence of abundant rates of protons and alphas, a rotating priority preference scheme was used to focus primarily on the more interesting medium and heavy nuclei. Those rate channels corresponding to heavy nuclei such as  $\text{Fe}^{56}$  were assigned to priority level I, intermediates such as the CNO group to priority II, and the alpha and proton channels to priority III. Rotation of this system always assigns highest priority preference to a group other than the last event transmitted. This arrangement is illustrated in the following table:

Last Event	Priority Order
III	I, II, III
II	III, I, II
I	II, III, I



Table 2-3 PHA I.D. Word

	Rate Ch	Octal Value	B1 MSB	B2	B3	B4	B5	B6	B7	B8 LSB
D1-D2 (D1a/D1b)	R1	040/140	0	0/1	1	0	0	0	0	0
	R2	041/141	0	0/1	1	0	0	0	0	1
	R3	042/142	0	0/1	1	0	0	0	1	0
	R4	043/143	0	0/1	1	0	0	0	1	1
	R5	020/120	0	0/1	0	1	0	0	0	0
	R6	021/121	0	0/1	0	1	0	0	0	1
	R7	022/122	0	0/1	0	1	0	0	1	0
	R8	060/160	0	0/1	1	1	0	0	0	0
	R9	061/161	0	0/1	1	1	0	0	0	1
D2-D3	R10	x44	x	x	1	0	0	1	0	0
	R11	x45	x	x	1	0	0	1	0	1
	R12	x46	x	x	1	0	0	1	1	0
	R13	x47	x	x	1	0	0	1	1	1
	R14	x23	x	x	1	0	0	1	1	1
	R15	x24	x	x	0	1	0	1	0	0
D5-D4	R43	x62	x	x	1	1	0	0	1	0
	R16	340	1	1	1	0	0	0	0	0
	R17	341	1	1	1	0	0	0	0	1
	R18	320	1	1	0	1	0	0	0	0
	R19	321	1	1	0	1	0	0	0	1
	R20	322	1	1	0	1	0	0	1	0
	R21	360	1	1	1	1	0	0	0	0
	R22	361	1	1	1	1	0	0	0	1
	R23	342	1	1	1	0	0	0	1	0
	R24	343	1	1	1	0	0	0	1	1
	R25	325	1	1	0	1	0	1	0	1
D3-D4 D1-D2 (D1c)	R26	364	1	1	1	1	0	1	0	0
	R27	351	1	1	1	0	1	0	0	1
	R28	350	1	1	1	0	1	0	0	0
	R29	326	1	1	0	1	0	1	1	0
	R30	370	1	1	1	1	1	0	0	0
	R31	x52	x	x	1	0	1	0	1	0
	R32	241	1	0	1	0	0	0	0	1
	R33	240	1	0	1	0	0	0	0	0
	R34	220	1	0	0	1	0	0	0	0
	R35	221	1	0	0	1	0	0	0	1
R36	260	1	0	1	1	0	0	0	0	

### 3.0 LEMPA System

The Low Energy Magnetospheric Particle Analyzer (LEMPA), designed primarily for planetary encounter measurements, includes eight detector elements. The sensor design is a complex arrangement including magnetic deflection, absorption shields, and scattering surfaces to permit analysis of electrons, protons and ions over very wide ranges of intensities and energies. The system is depicted in Figure 3.1.

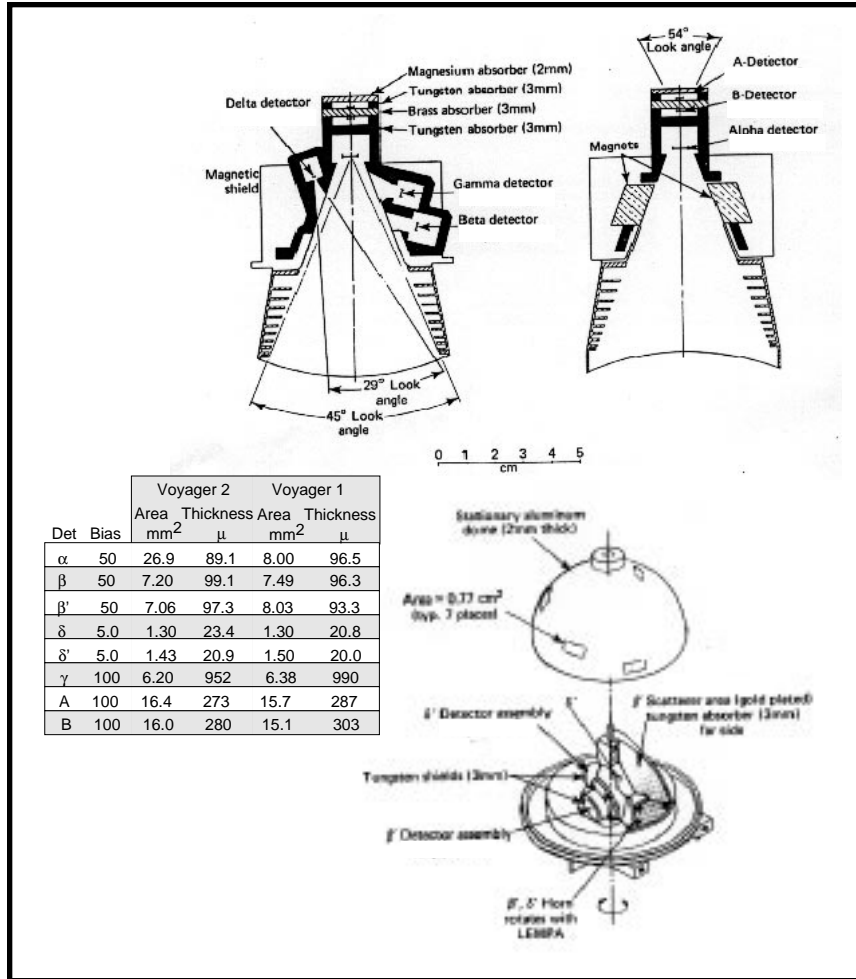


Figure 3.1 LEMPA Sensor Assembly

Some of the circuitry for processing the LEMPA signals is similar to circuitry used in the LEPT system. In general, however, the requirements for the LEMPA measurements were quite different from those for LEPT, and this led to the development of different circuit configurations and the design of several additional hybrid modules. The electronic designs for each of the LEMPA channels are described in some detail below.

### 3.1 Alpha Channel

The alpha detector analyzes protons and ions entering the front aperture of the LEMPA sensor. The electronic design reflects the need for lowest noise operation (consistent with the detector size and counting rate requirements), in order to extend the sensitive range down to minimum energies. In fact we were able to achieve a minimum detection threshold of 12 keV. A schematic representation of the channel design is given in Figure 3.2.

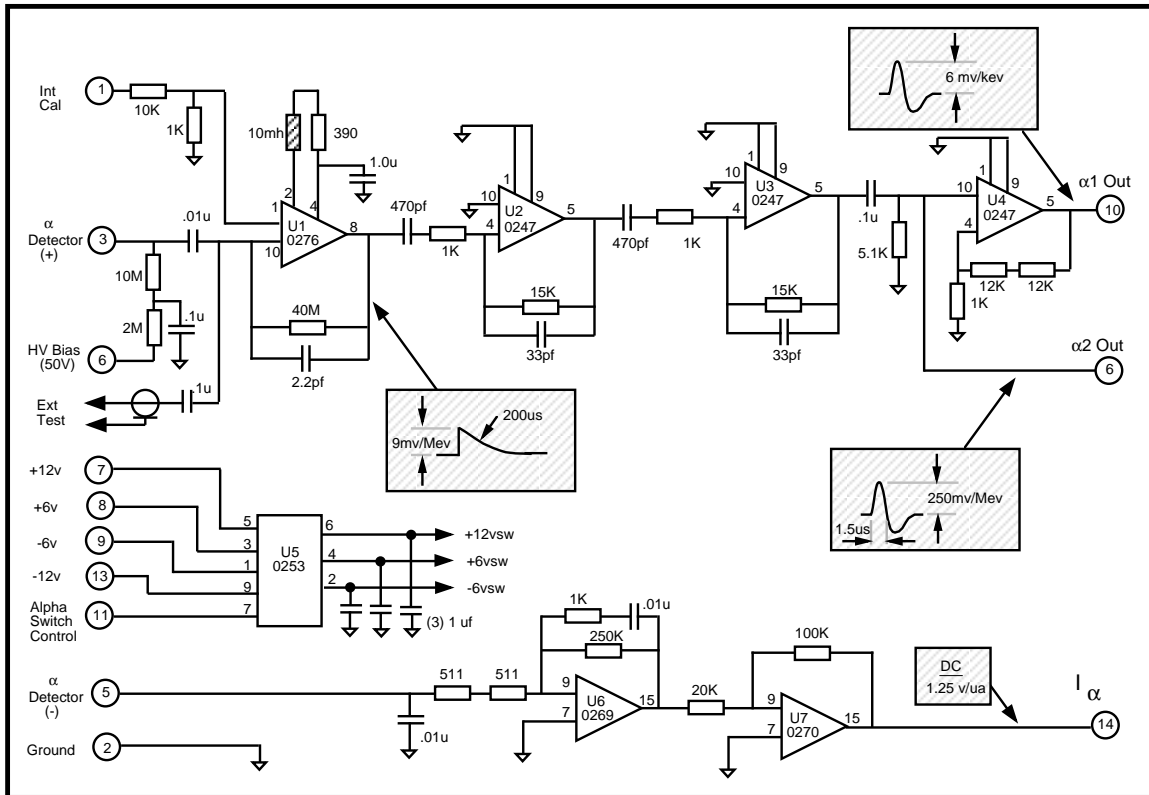


Figure 3.2 Alpha Channel

The preamplifier is essentially identical to that used in the LEPT system, with the exception of the front end field-effect transistor. The JFET chosen for the alpha channel, while somewhat lower in transconductance, offered considerably lower gate-to-channel capacitance and this was essential in maintaining overall noise to minimum level. The shaping amps were the same 0247 hybrids used extensively in the LEPT system. Double RC differentiation with double RC integration was used, with all time constants set at 500 ns, yielding a zero-crossover at 1.5  $\mu$ s. Although slightly better noise performance could have been attained with unipolar pulse shaping, this would have necessitated an active baseline restorer; such a system would have consumed added space and power and could have compromised reliability in a long-life mission such as Voyager. These complications were avoided by the selection of double-differentiating filters, which permit ac coupling between the low and high gain output stages and to the discriminators as well.

The high and low gain pulse outputs from the analog board were transmitted down the polytwist into banks of discriminators located in the Pulse Circuits Assembly in the LECP fixed section. Ten discrimination thresholds were implemented, using the 0262 hybrid modules described previously. Those driven from the third (or high-gain) analog stage were designated  $\alpha 1-0$  through  $\alpha 1-4$ ; those driven from the second stage were  $\alpha 2-0$  through  $\alpha 2-4$ . The  $\alpha 1-0$  threshold was command-selectable between two values, in order to provide margin in the event of degraded noise performance due to radiation damage, temperature increases, or other calamities that might occur during the mission. The discriminators were combined into ten differential window channels by means of extremely simple hold/strobe circuitry implemented with diode isolated RC relaxation networks. These channels and their measured electronic passbands are summarized in Table 3-1 below. Note that the figures in this table do not take account of energy loss due to dead layer and pulse height defect, which are of considerable importance here in view of the extremely low threshold settings. True energy bandpasses, including these effects, were established by particle beam calibration and reported by *Krimigis et al, 1981*.

	VOY2 SN01	SN02	VOY1 SN03
P $\alpha$ 1	12-31keV	14-34	14-31
P $\alpha$ 2	31-62	34-68	31-63
P $\alpha$ 3	62-114	68-136	63-121
P $\alpha$ 4	114-200	136-216	121-200
P $\alpha$ 5	200-528	216-520	200-550
P $\alpha$ 6	528-982	520-1.04	550-1.05
P $\alpha$ 7	982-2.14 MeV	1.04-1.95	1.05-2.0
P $\alpha$ 8	2.14-4.0	1.95-4.0	2.0-3.93
A $\alpha$ 1	4.0-7.44	4.0-7.0	3.93-7.13
A $\alpha$ 2	>7.44	>7.0	>7.13

Table 3-1 Alpha Detector Channels

An additional feature of the alpha channel provides direct measurement of detector current. This was implemented by returning the back side of the detector to the virtual ground of an operational amplifier configured as a transresistance converter, as shown in the lower section of Figure 3.2. After suitable voltage gain this dc reading is presented to the PHA with a scale factor of 1.25 v/ $\mu$ A and read out in telemetry. The reading obtained in this manner continues to provide an accurate measurement of the rate of energy deposition in the alpha detector out to flux rates that are at least two orders of magnitude beyond the point of saturation in the pulse counting circuitry. This feature proved extremely useful during the Voyager 1 encounter with Jupiter, when the alpha detector channel was overwhelmed by enormous fluxes of ions (now believed to be primarily O<sup>n+</sup>). This resulted in both linear pileup of the bipolar signals and a baseline shift at the  $\alpha 1$  output arising from unequal saturation characteristics of the positive and negative pulse lobes. The data were eventually rationalized with the help of laboratory studies of the baseline shift characteristics, performed on the flight spare. Details and results of this analysis were reported by *Mauk et al, 1996*.

### 3.2 Beta and Gamma Channels

Electrons entering the LEMPA main aperture are deflected by the magnetic field into the beta and gamma detectors. The low energy portion of the electron spectrum is counted in beta. The electronic system supporting this detector is essentially identical to that of the alpha channel described above, including the direct measurement of detector current and a minimum detection threshold of 12 keV. The pulse signals are analyzed by five discriminators and assigned to five differential windows designated E $\beta$ 1-E $\beta$ 5, with measured electronic passbands as given in Table 3-2.

	VOY2 SN01	SN02	VOY1 SN03
E $\beta$ 1	12-35 keV	16-33	15-34
E $\beta$ 2	35-61	33-66	34-67
E $\beta$ 3	61-112	66-125	67-125
E $\beta$ 4	112-183	125-210	125-190
E $\beta$ 5	>183	>210	>190

Table 3-2 Beta Detector Channels

E $\gamma$ 6	>250 keV
E $\gamma$ 7	>500 keV
E $\gamma$ 8	> 1 MeV
E $\gamma$ 9	> 2 MeV

Table 3-3 Gamma Detector Channels

The gamma channel is designed for intermediate energies and significantly higher counting rates. Because the speed required is near the upper limit of that which can be obtained using the LEPT hybrid circuits, additional amplifier and discriminator modules were designed for this channel and others (see below) in the LEMPA system. The channel design is given schematically in Figure 3.3. The signals detected by the gamma detector are assigned to four integral channels designated E $\gamma$ 6-E $\gamma$ 9, with nominal thresholds listed in Table 3-3. True energy bandpasses for both the  $\beta$  and  $\gamma$  channels must take account of not only dead layer effects but also the selection effects associated with the magnetic deflection field. These effects have been summarized by *Krimigis et al, 1983* and by *Mauk et al, 1987*.

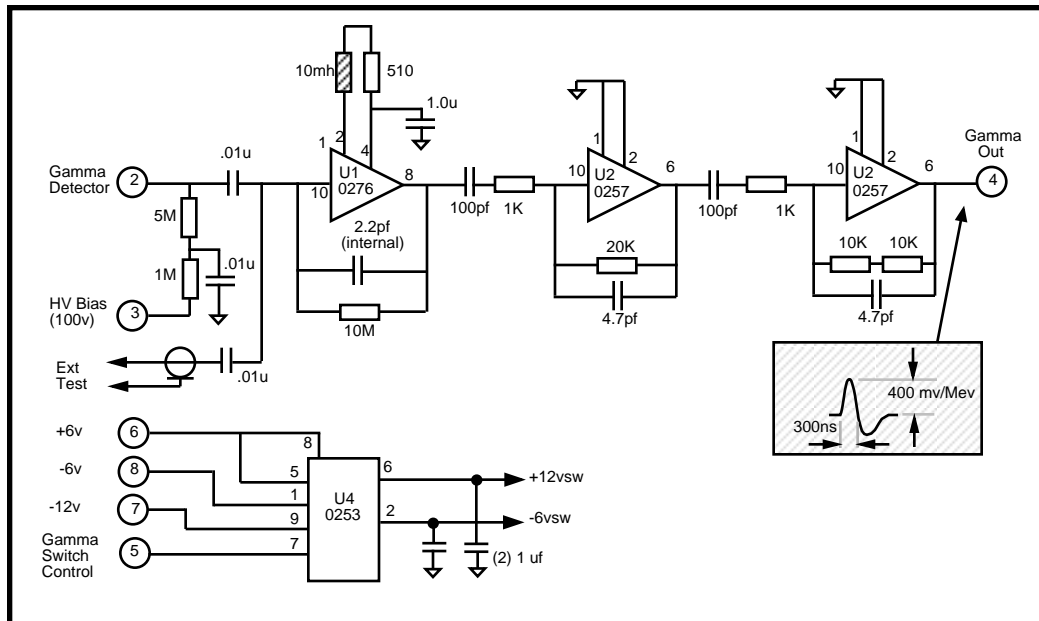


Figure 3.3 Gamma Channel

### 3.3 Beta Prime

The  $\beta'$  detector is located in the portion of the LEMPA sensor assembly lying under the stationary aluminum dome, with a field of view perpendicular to the ecliptic plane. This detector has its own preamp and first stage shaping amplifier; beyond this point its signal is time-multiplexed with that of the beta detector under control of the FDS clock.

### 3.4 A,B Channels

The channels designated A and B are included for high intensity, high energy measurements during the planetary encounter phases of the Voyager mission. Their design, illustrated in Figure 3.4, takes specific account of the enormous electron fluxes expected during the encounters, minimizing primary pile-up effects by the use of extremely fast analog shaping with primary lobe crossover at 50 nanoseconds. In order to meet this need, additional special purpose hybrids were developed. These designs (EME0257 linear amp and EME0277 pulse height discriminator) are described in Section 4.5 of this document. The A and B thresholds are set primarily by the magnesium and brass absorbers in front of the detectors (see Figure 3.1).

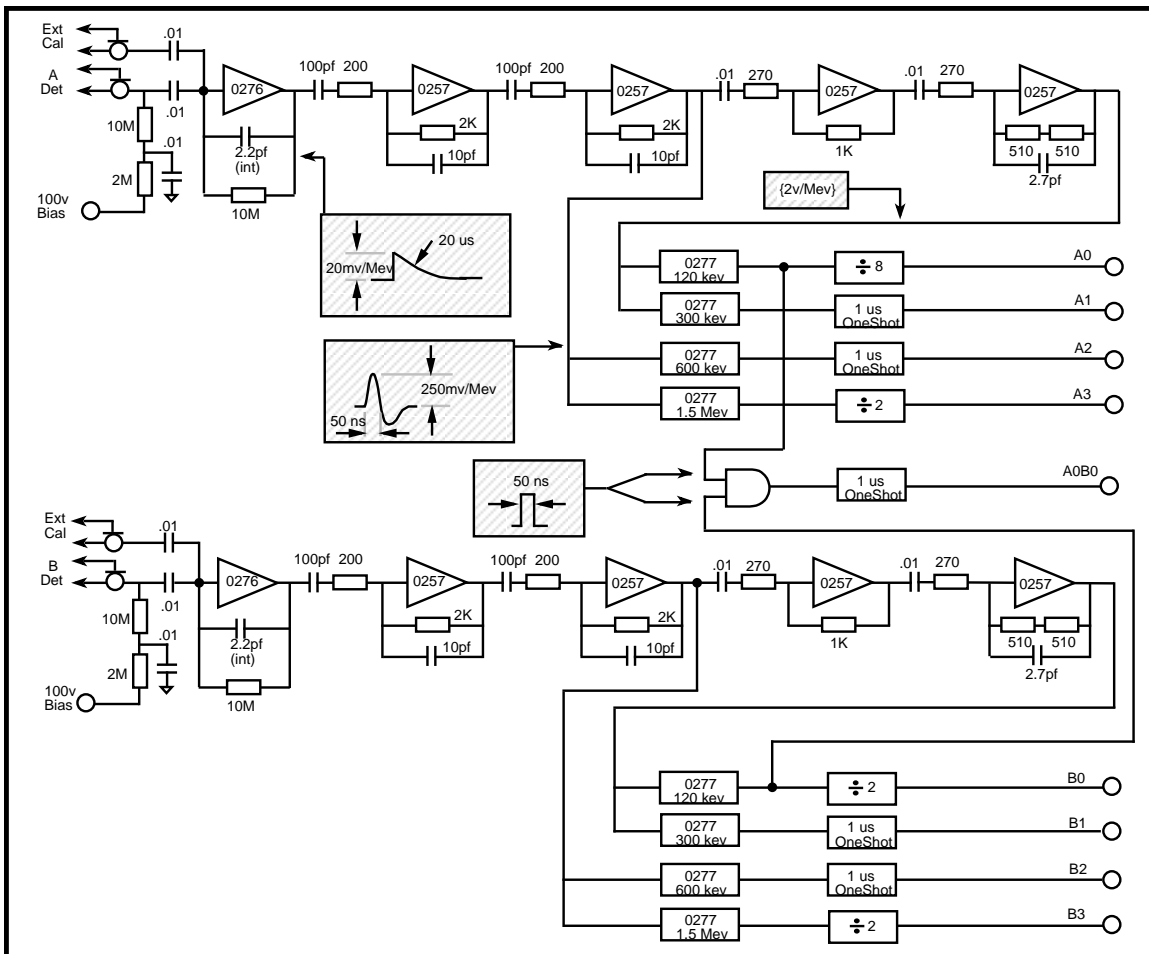


Figure 3.4 A & B Channels

### 3.5 Delta, Delta Prime Channels

The delta detector, located in the main LEMPA sensor section, looks out over a field of view centered slightly off center with respect to the telescope main axis. The 29 degree field is defined by the thick tungsten shielding. The  $\delta'$  detector is located under the stationary dome (along with the  $\beta'$  detector) in order to gather three-dimensional pitch angle distributions. Each of the two detectors has its own charge-sensitive preamplifier. The signals from these two preamps are time multiplexed into a common main filter/amp combination under control of the same FDS line that controls  $\beta, \beta'$  selection.

These channels provide the highest intensity proton and alpha measurements in the LEMPA system. Optimized for perijove operation at  $\sim 5 R_J$ , the detectors are 1 mm<sup>2</sup> in area. The delta channel electronics make use of the same hybrid pair as the A,B channels but with considerably faster shaping times. Scope photos of the output amp and discriminator signals are illustrated in Figure 4.7; schematic representation is given in Figure 3.5. The second filter stage drives six discriminators in parallel, each of which is scaled down by a factor of two in rate. The resulting integral channels and their nominal thresholds are summarized as follows:

P $\delta$ 9	>250 kev
P $\delta$ 10	>400 kev
P $\delta$ 11	>700 kev
A $\delta$ 3	>1.7 Mev
A $\delta$ 4Z	>2.5 Mev
Z $\delta$ 1	>6.0 Mev

Table 3-4 Delta, Delta' Detector Channels

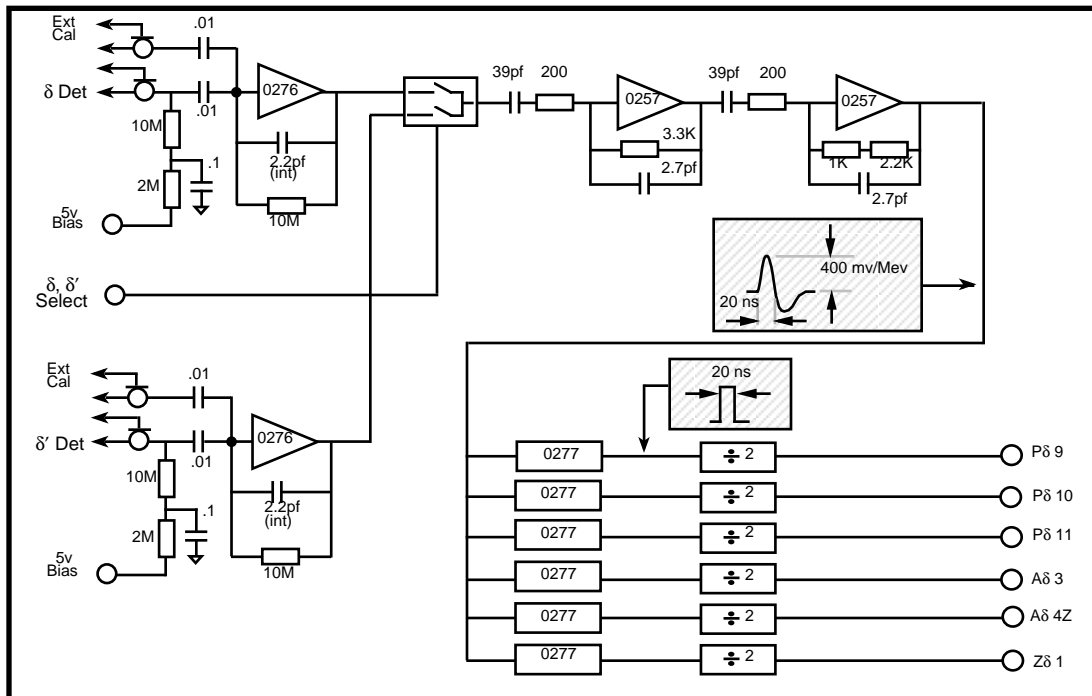


Figure 3.5  $\delta, \delta'$  Channels

## 4.0 Hybrid Circuits

As discussed in the introduction to this document, the LECP electronic design was largely based on a family of hybrid microcircuits developed specifically for this instrument. Some of these were used extensively in subsequent instruments as well. This section will present the design features of several of the more interesting ones.

### 4.1 Linear Amplifier (0247)

The 0247 was a general purpose linear amplifier designed to meet specific requirements of bandwidth, power consumption and differential offset imposed by the LECP constraints. It was used throughout the LEPT and LEMPA systems to perform the functions of voltage gain, pulse filtering and signal summation.

The design was based on the use of monolithic bipolar transistor and diode arrays, taking advantage of the density and, most importantly, the component matching characteristics afforded by this technology. The schematic is shown in Figure 4.1. Transistors Q1 and Q2 form a differential input pair driving a common base stage Q6. The Q6 collector is connected to a high dynamic impedance load to provide excess voltage gain while the transistors Q3 and Q7-Q10 constitute a complementary emitter follower to provide a low bi-directional open loop output impedance.

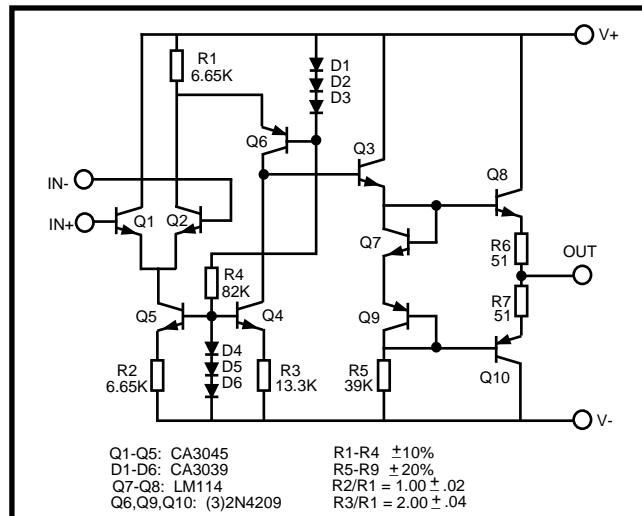


Figure 4.1 Hybrid Linear Amplifier, EME0247

The input section is biased by a pair of tightly matched current sources Q4 and Q5. These are in the ratio 2:1, as determined by the resistances of R2 and R3. Nominal current values are 200ua through Q5 and 100ua in Q4. Note that although the absolute tolerance on the resistors was 10%, the tolerance on their ratio was 2%, well within the range of thin film technology. The 5mv maximum differential (0.5mv typical) in the base-to-emitter voltages of Q4 and Q5 contributes a worst case error in the current ratio of less than 5%, so that the current balance was limited almost entirely by the matching tolerance on the resistors. The bias circuit of Q6 is complementary to that of Q5. The three series diodes are of the same monolithic array as those in the lower current pair



and the Q6 emitter is connected to a resistor R1 matched to R2 by the same 2% ratio tolerance. The current in R1 is thus 200ua; half of this is drained by Q4 leaving 100ua for the collector of Q2. Since the Q5 current is fixed at 200ua, 100ua comes from Q1, thereby balancing the input pair. The largest error in this balance arises from the inherent mismatch of the PNP transistor Q6 with respect to the NPN current sources. Its characteristics are such however that the difference in base-to-emitter voltage between Q6 and Q5 is unlikely to exceed 50mv. Since the overall drop across R1 or R2 is around 1400mv, this leads to no more than a 3% error in the Q6 to Q5 current ratio. Adding this to the 2% mismatch in the R2/R3 ratio and a similar 2% in the R1/R2 ratio yields an overall maximum error in the Q1 to Q2 current balance of 14%. This corresponds to an input voltage offset of no more than 3.4mv, exclusive of the inherent offset in the input transistor pair.

In fact, the measured offsets for the completed units showed 55% holding better than 2mv, with 95% below 5mv. The hybrid design provides adjustment points at pins 6 and 8, allowing a single external resistor to null the residual offset to <1mv. The board layouts accomodated this provision in those applications where this adjustment was important.

Dynamic characteristics are summarized by the open-loop frequency response curves of Figure 4.2. These show a low frequency voltage gain of 2000, a first break point at 20Khz and a secondary break at ~16Mhz. Analysis of the two-pole model leads to critical damping at a closed loop gain setting of x10, with a non-overshoot rise time (10-90%) of 70ns. This provided more than adequate speed margin for all the LEPT channels and for the LEMPA alpha and beta channels.

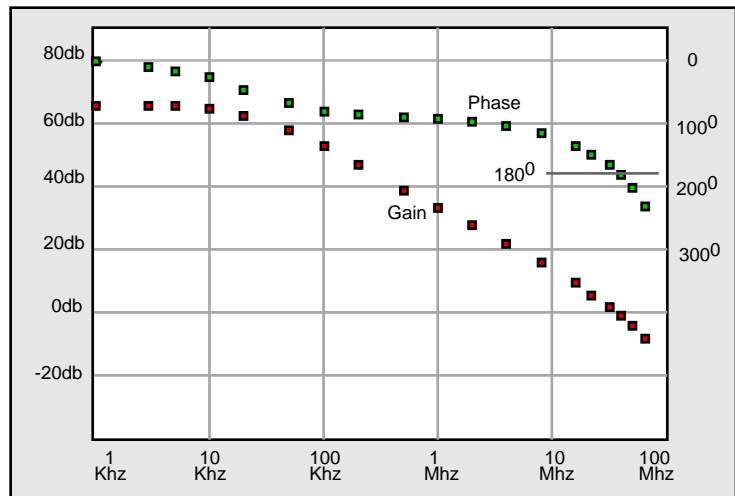


Figure 4.2 Gain And Phase vs. f, EME0247

The amplifier current drain was 0.8 ma from each of the power supply lines when operated with balanced 6v supplies, for an overall drain of 9.6 mw. When operated at +12v and -6v, as in the LEPT D3 and D4 channels, the power increased to 16 mw.

## 4.2 Logarithmic Amplifier (0254)

Logarithmic conversion in the LEPT system was performed by the 0254 hybrid, specifically developed to meet the requirements of the wide range signals from the D1-D5 detectors. These requirements were discussed in Sections 2.1 and 2.2. The logarithmic response derives from the connection of a bipolar transistor as the feedback element across an operational amplifier. The basic circuit is in some respects a variation on the design theme of the 0247 linear amplifier, consisting of a balanced differential pair driving a pnp common-base stage, followed by a complementary emitter follower. The input stage in this case is an n-channel JFET pair and the entire circuit depends on matched current sources synthesized from monolithic arrays and transistor pairs. The schematic is given in Figure 4.3.

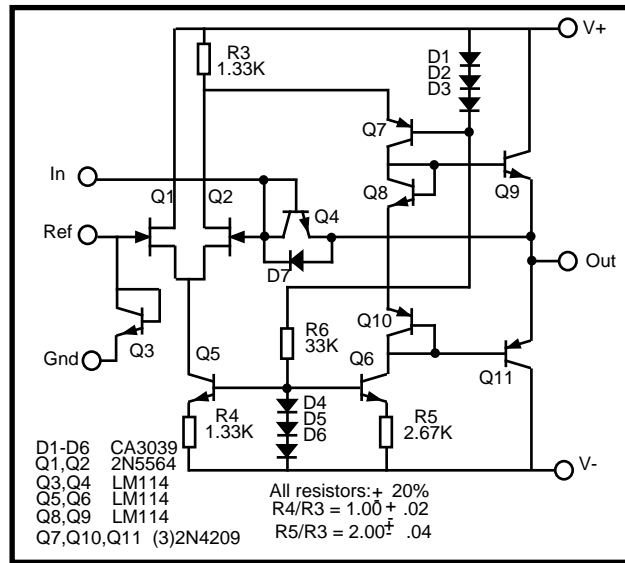


Figure 4.3 Hybrid Logarithmic Amplifier, EME0254

Transistors Q5 and Q6 form a pair of current sources supplying 1.0 and 0.5 ma respectively, while the current through R3 is held at 1.0 ma. Error analysis is similar to that given above for the 0247. With an assumed FET transconductance of 5 ma/v, the computation yields a maximum offset of 14 mv in addition to the inherent 5 mv offset for the input JFET pair. Testing of the actual hybrids (several dozen units spread over three programs) showed more than half exhibiting offsets of under 6 mv, and 85% under 10 mv. As in the 0247, adjustment trim points were brought out to allow nulling of the residual offset with a single external resistor.

The transistor Q4 was used as the logarithmic element, diode-connected between the output and the inverting input terminals. The matching transistor Q3 was similarly connected between the reference input and ground. Equal reference currents are supplied through each of these through precision external resistors, so that the deviation of the output dc level, arising from the offset between Q3 and Q4, is <0.5 mv and negligible for these measurements.

### 4.3 LEPT Pulse Height Discriminator (0262)

The discriminator hybrid, shown in Figure 4.4, consists of an operational transconductance amplifier and three CMOS inverters, with two discriminators to a hybrid module. The positive reference voltage is established by the feedback resistor R2 and an external resistor connected between the pin 1 reference point and ground. When the incoming analog signal exceeds the reference, the OTA output swings positive and the negative-going transition of the first inverter feeds back to the reference input. The action is regenerative, resulting in the output going to the positive rail and the reference being driven to zero volts. The reverse sequence takes place when the input passes through zero on its downward swing, thereby restoring the circuit to its standby state.

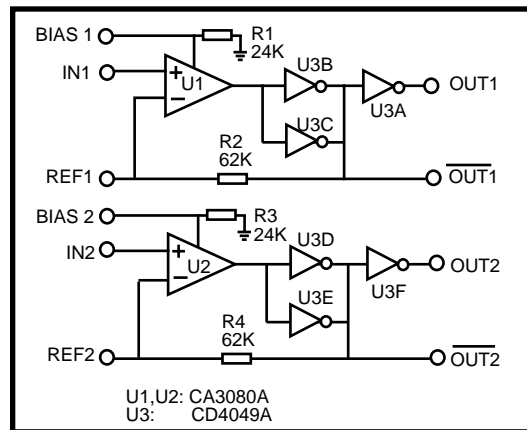


Figure 4.4 Hybrid Dual Discriminator, EME0262

The speed of the discriminator is limited by the OTA bias current, which is determined by the resistor R1. This current is 250  $\mu\text{A}$ , resulting in an operating delay of about 1  $\mu\text{s}$  measured from the time the input reaches threshold until the output transition is halfway complete. This delay is reduced to about 500 ns for large input signals where the input is strongly overdriven. The design contains provision for increased speed by means of an externally connected resistor in parallel with R1, and this feature is used in the five discriminators corresponding to the lowest thresholds in each of the D1-D5 channels. The trailing edge of each of these discriminators is used as a timing reference, and the increased speed resulting from the higher bias current tends to stabilize the delay against variations in signal level.

#### 4.4 Dual One Shot (EME0263)

The timing circuitry used in the LEPT rate logic control sequence is based on the use of the 0263 dual one-shot hybrid. These are simple circuits, packaged two to a module, each consisting of an OTA and a D-type flip-flop, with complementary outputs. The pulse width for each one-shot is determined independently by means of one externally connected capacitor. The module and the calibration curve are illustrated in Figure 4.5:

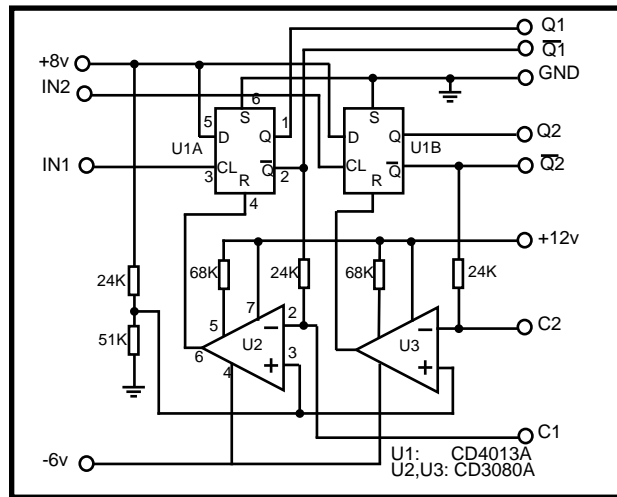


Figure 4.5a Hybrid Dual One Shot, EME0263

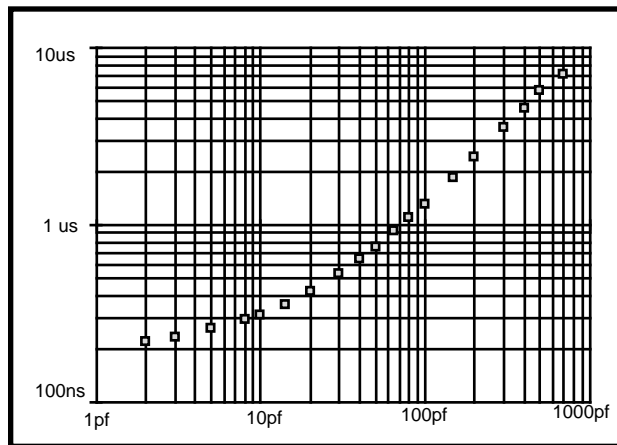


Figure 4.5b Pulse Width vs External Capacitance  
EME0263 Dual One Shot

#### 4.5 Fast Linear Amplifier and Fast Discriminator (0257 and 0277)

The LEMPA detector channels designed for planetary encounter required the ability to resolve extremely high counting rates, well beyond those that could be handled by the circuits described above. In order to meet this need a special pair of modules was developed, with the emphasis on speed rather than precision. These were the 0257 amplifier and the 0277 discriminator, used throughout the A, B,  $\delta$  and  $\delta'$  channels. They are shown schematically in Figures 4.6 and 4.8. A waveform pair taken from an ancient oscilloscope trace is reproduced here as Figure 4.7, illustrating the speed of response actually attained in the delta channel (yes, there were cameras in those days).

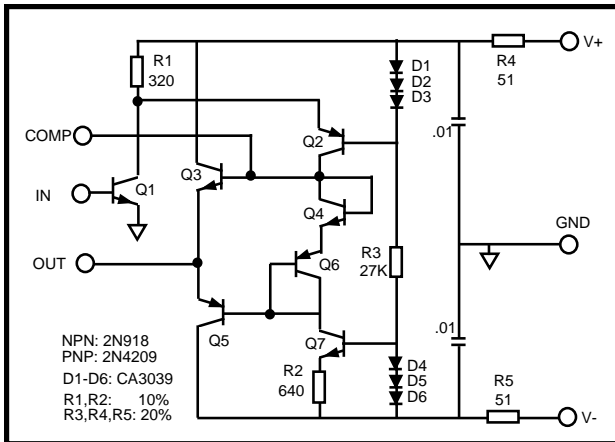


Figure 4.6 Hybrid Fast Amplifier, EME0257

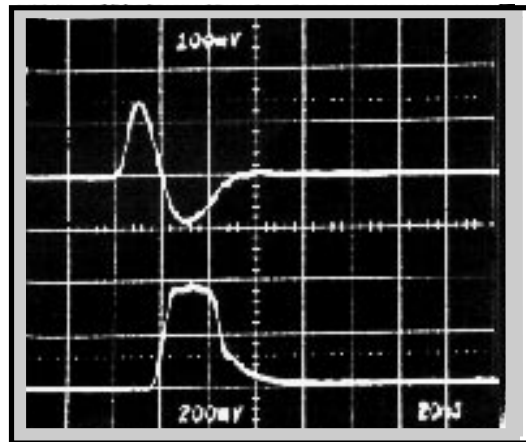


Figure 4.7 Delta Channel Waveforms

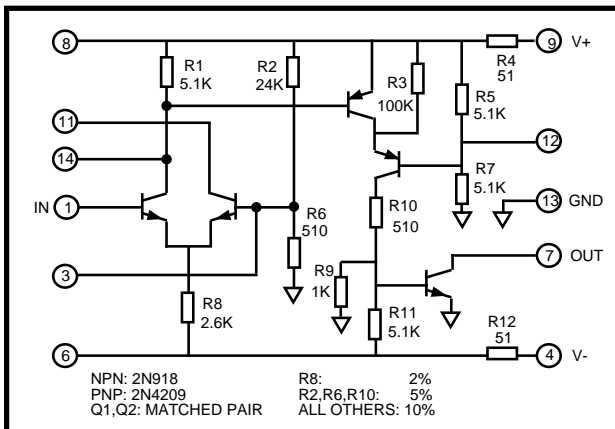


Figure 4.8 Hybrid Fast Discriminator, EME0277

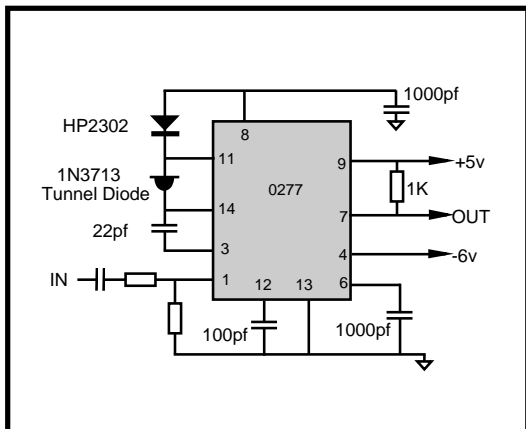


Figure 4.9 0277 External Connections

## **5.0 Commands, Operating Modes and Formats**

The LECP was designed for three normal modes of operation, corresponding to the three distinct environments in which it was to perform. In interplanetary space, the composition and anisotropy measurements on particles of solar and galactic origin are paramount and the instrument operated in one of several Cruise Modes, with the majority of its telemetry allocated to PHA data and the remainder to rate channels. During the transition from interplanetary space to the vicinity of planetary magnetospheres the LECP operated in Far Encounter Mode, in which the telemetry allocation was altered so that two thirds was assigned to the rate channel data. For these encounters, the bit rate was increased to 600 bits per second. Finally, during the period when the Voyager spacecraft were within the intense trapped radiation regions associated with the Jovian environment, the LECP operated in Near Encounter Mode with the LEPT system entirely off, the LEMPA system fully operational and the data format reassigned to reflect this mode of operation.

### **5.1 Command Structure**

The instrument state is controlled by a set of 40 On/Off commands, arranged as four 12 bit command words. The two most significant bits of each word denote the word address, while the remaining ten bits of each word control the state of individual binary switches within the instrument. These commands are listed in Table 5-1.

### **5.2 Operating Modes**

In Cruise Mode the LEPT system is fully on and the  $\alpha$ ,  $\beta$ ,  $\beta'$  and  $\gamma$  detectors of the LEMPA system are operational. Rate channel data are arranged in seventeen groups with each group consisting of four 10-bit words. Each of these words represents a log compressed expression of the accumulation total in a 24-bit counter assigned to that rate channel. The last two words of group 16 and all four words of group 17 are allocated to instrument status rather than data. The Cruise Mode groups are summarized in Table 5-2. The modes designated Cruise 1 through Cruise 6 were used at various stages of the Voyager mission, following a common data format summarized in Table 5-3. Under this format the telemetry consists of 200 blocks arranged in an 8 x 25 array, where each block contains two PHA events and one of the rate channel groups listed in Table 5-2. A single block thus contains 120 bits of data (40 bits for each of the two PHA events, and 40 bits for the rate channel group). These operating modes differed in bit rate, which ranged from 250 bps allocated to the LECP in Cruise 1 mode to 16 2/3 bps in Cruise 6. This of course entails a corresponding inverse variation in the channel accumulation times. In all of these modes, the motor step rate was one sector every 6 minutes.

The Cruise 5A mode has been in effect for both Voyager spacecraft since the summer of 1990, about one year after the Voyager 2 Neptune encounter. This mode uses an entirely different format, summarized at the bottom of Table 5-3. Half of the 64 blocks in the record are allocated to PHA data. The motor step rate is one sector every 192 seconds, synchronized to the first PHA readout in the sequence.

For the Far Encounter Mode, a different data format was used, reflecting the importance of the distant planetary magnetospheres. This format is presented in Table 5-4, showing the data arranged in an 18 x 20 array. Here each block represents either a single PHA event or an individual rate channel group. Again, a PHA event takes 40 bits

and each rate channel group takes 40 bits. The whole sequence consists of 14,400 bits read out at 600 bps, requiring 24 seconds to complete. The motor steps one sector in each of these 24 second intervals.

The Near Encounter Mode in effect reconfigured the LECP for the different kind of environment expected deep in the Jovian magnetosphere. The LEPT system was turned off entirely and the remaining LEMPA channels (A, B,  $\delta$  and  $\delta'$ ) were turned on. The data format deletes all LEPT channels and adds additional channel groups corresponding to the now active LEMPA detectors. The Near Encounter rate channel groups are summarized in Table 5-5. The data format, given as Table 5-6, is an 18 x 10 array where each block represents a rate channel group of four 10-bit words. These are read out at 600 bps, requiring 12 seconds to read the full sequence. In this mode, the motor scan rate was one sector in each 12 second sequence.

### 5.3 Status Words

Included within the LECP data stream are six 10-bit status words, designated S1 through S6, reporting the operating state of the instrument. In Cruise and Far Encounter modes, these are read out once per major frame as the last two words in Rate Group 16 and as the four words of Group 17. In Near Encounter mode, they are read out as the last two words of Group 17, subcommutated so that four frames are required to read the full set. The respective positions of these words in the Rate Groups and the order of subcommutation are listed in Tables 5-2 and 5-5.

The first four of these status words confirm the LECP command state, echoing the last commands received and executed. The S5 word indicates motor position and the state of the frame counter. The S6 word tracks the advance of the analog multiplexer, the subcommutation within Rate Groups 4 and 8, and the state of the  $\beta, \beta'$  multiplexer. A full summary of these status words is given in Table 5-7.

### 5.4 Scanning System

The stepper motor system rotates the upper section of the LECP in 45 degree increments, with each sector change initiated by a trigger supplied from the spacecraft Flight Data System. In Cruise Mode 5A and in both the Far Encounter and Near Encounter modes, the changes are initiated at the beginning of the frame readout (upper left corner in Tables 5-3, 5-4 and 5-6). Following these sector changes, which take approximately 0.5 seconds to complete, the system remains fixed in position until the next FDS trigger. An optical encoder system monitors the position of the stepper base, reporting the position in the first four bits of status word S5. Interpretation of this readout is as described in Table 5-7.

Because of the polytwist connections between upper and lower sections, the scanning system is restricted to 360° of motion, so that continual scanning involves reciprocation between the two rotational directions. The eight viewing sectors are designated sectors 1 through 8 and the normal scanning sequence is thus:

8-7-6-5-4-3-2-1-1-2-3-4-5-6-7-8-8-7-6-.....

Note that a double dwell period occurs at the end sectors 1 and 8, in order to equalize the accumulation intervals for all look directions. A limited scan sequence, used only for

post-launch near earth operations, omitted viewing in sector 1 entirely and provided a double dwell period and reversal at sector 2.

The system is powered by a bank of forty-eight 270  $\mu\text{f}$  capacitors connected in parallel, trickle charged between sector changes directly from the spacecraft 30 volt supply. By this means the energy surges required to change position quickly are isolated from the S/C power system. Under normal operation the recharge time constant is eight seconds. This recharge time can be reduced to two seconds by means of the Accelerated Motor Step Rate command in the listing of Table 5-1 (Command Word #3, bit 8).

Several special options were designed into the scanning system in order to take account of possibilities only vaguely foreseeable prior to launch. Among these are the following:

a) Cease Scanning

The stepper can be ordered to cease scanning and remain indefinitely in any chosen sector by means of CW #3, bits 9-12. Bit 9 activates the Mot to Cmd Pos command, while bits 10-12 denote the sector to be retained. Following reset of bit 9, regular scanning is resumed as if no interruption had occurred.

b) Increased Power

The motor normally operates in its lowest power mode. However, we considered the possibility that the system might begin to display some obstinacy, perhaps as a result of wear. For this reason the Motor Drive Pwr command is available as CW #3, bit 7. Activation of this command has the effect of increasing the drive pulse duty cycle, thereby achieving maximum torque at the expense of increased power.

c) Emergency

An emergency mode has been included, for use in the event that neither the low nor the high power mode succeeds in driving the stepper base. This mode is enabled by CW #3, bit 6. Its effect is to reduce the motion arising from each FDS trigger to  $1.8^\circ$ , so that twenty-five trigger pulses are required to bring about a  $45^\circ$  sector change.

d) 60 Hz Operation

During sector changes, the motor normally operates at a 50 Hz pulse rate generated by a clock within the LECP. This rate can be increased to 60 Hz by exercising CW #3, bit 3. This feature was included to take account of possible vibrational resonances or interference with the Voyager spacecraft or other instruments. It has not been necessary to use this option during the mission.

## 5.5 In Flight Calibrator

The LECP includes an In Flight Calibration (IFC) system to run diagnostic checks on the analog systems. The central element of the IFC is a variable-amplitude pulse generator which injects test signals directly into the charge preamps in parallel with the detector signals. The outputs of the LEPT discriminators and the LEMPA  $\alpha$  and  $\beta$  channels are routed to a 60 channel multiplexer, allowing sampling of one discriminator at a time. The selected discriminator is probed in synchronism with the pulse generator clock, and the relative rate of discriminator firings compared with the clock rate. The reference voltage of the pulse generator is continuously increased or decreased accordingly, seeking a stable level. Owing to the gaussian distribution of system noise, the difference in the pulse amplitudes corresponding to the 12% and 88% response points provides a direct measure of the FWHM channel noise; the mean of these two



amplitudes of course measures the 50% response point and represents the discrimination threshold. Two readings of the calibrator are therefore taken at each multiplexer position. A gate signal generated by the IFC clock blanks all rate logic inputs for a 10  $\mu$ s interval at each pulse in order to preclude contamination of the detector data by the test signals.

The calibrator system is turned on and off via uplink command (Word 4, bit 10). The discriminator select multiplexer steps to its next position every 12 seconds in response to a pulse from the FDS, while the pulse generator reference voltage is read by the spacecraft and downlinked as Subsystem Engineering Measurement E-451. The full calibration sequence takes 24 minutes to complete. The system has been operated on a periodic basis since launch at intervals varying from weekly during the earlier phases of the mission to once every few months in recent years.

Table 5-1. LECP Commands

			0	1	
Command Word #1	LSB	12	LEPT, AC1&AC2	Off On	
		11	LEPT, AC3&AC4	Off On	
		10	LEPT, AC5&AC6	Off On	
		9	LEPT, AC7&AC8	Off On	
		8	LEPT, D1a	Off On	
		7	LEPT, D1b	Off On	
		6	LEPT, D1c	Off On	
		5	LEPT, D2	Off On	
		4	LEPT, D3	Off On	
		3	LEPT, D4	Off On	
		2	Address	0 x	
		MSB	1	Address	0 x
				0	1
Command Word #2		12	LEPT, D5	Off On	
		11	LEMPA, $\alpha$	Off On	
		10	LEMPA, $\beta, \beta'$	Off On	
		9	LEMPA, $\gamma$	Off On	
		8	LEMPA, $\delta, \delta'$	Off On	
		7	LEMPA, A	Off On	
		6	LEMPA, B	Off On	
		5	Spare	Off On	
		4	High Bias	Off On	
		3	Low Bias	Off On	
		2	Address	x 1	
		1	Address	0 x	
				0	1
Command Word #3		12	Mot Pos Bit 1	Off On	
		11	Mot Pos Bit 2	Off On	
		10	Mot Pos Bit 3	Off On	
		9	Mot to Cmd Pos	Off On	
		8	Acc Mot Step Rate	Off On	
		7	Mot Drive Pwr Increased	Off On	
		6	Emergency Mot Pwr	Off On	
		5	Full Mtr Scan	Off On	
		4	D1Fast Subcom (46,47)	Off On	
		3	Motor, 60 Hz	Off On	
		2	Address	0 x	
		1	Address	x 1	
				0	1
Command Word #4		12	Near Encounter	Off On	
		11	LEPT Low Disc	Off On	
		10	Calibrator	Off On	
		9	PHA Power	Off On	
		8	LEPT High Disc	Off On	
		7	Low $\alpha, \beta, \beta'$ Discs	Off On	
		6	Rates 44,45 Subcom	Off On	
		5	PHA Failure Mode	Off On	
		4	Rate Format Failure Mode	Off On	
		3	LEPT E1 Disc High	Off On	
		2	Address	x 1	
		1	Address	x 1	

Table 5-2. LECP Rate Channel Groups  
Cruise and Far Encounter Modes

Group Number	Rate Channels in Group			
1	P $\alpha$ 1	P $\alpha$ 2	P $\alpha$ 3	E $\beta$ 4
2	E $\beta$ 1	E $\beta$ 2	E $\beta$ 3	E $\gamma$ 6
3	39	33	32	31
4	E $\gamma$ 7	E $\gamma$ 8 / 44 #	E $\gamma$ 9 / 45 #	E $\beta$ 5
5	1	44	3	10
6	P $\alpha$ 4	P $\alpha$ 8	42	16
7	11	23	27	4
8	13 / 46 #	17 / 47 #	28	38
9	35	P $\alpha$ 5	P $\alpha$ 6	P $\alpha$ 7
10	45	41	12	24
11	34	5	18	14
12	6	7	19	36
13	8	43	25	9
14	29	22	26	30
15	A $\alpha$ 1	A $\alpha$ 2	37	21
16	15	20	S5	S6
17	S1	S2	S3	S4
	# Subcommutated	LEPT	LEMPA	Status

Table 5-3. Cruise Mode Data Formats, LECP

Cr 1-6	1	2	3	5	1	2	4	7
	1	2	3	6	1	2	4	13
	1	2	3	8	1	2	4	5
	1	2	3	9	1	2	4	6
	1	2	3	11	1	2	4	10
	1	2	3	5	1	2	4	7
	1	2	3	6	1	2	4	14
	1	2	3	8	1	2	4	5
	1	2	3	9	1	2	4	6
	1	2	3	12	1	2	4	10
	1	2	3	5	1	2	4	7
	1	2	3	6	1	2	4	15
	1	2	3	8	1	2	4	5
	1	2	3	9	1	2	4	6
	1	2	3	13	1	2	4	10
	1	2	3	5	1	2	4	7
	1	2	3	6	1	2	4	11
	1	2	3	8	1	2	4	5
	1	2	3	9	1	2	4	6
	1	2	3	16	1	2	4	10
	1	2	3	5	1	2	4	7
	1	2	3	6	1	2	4	12
	1	2	3	8	1	2	4	5
	1	2	3	9	1	2	4	6
	1	2	3	17	1	2	4	10

← 8 →

↑ 25 ↓

Cr 5A	P	P	P	P	P	P	P	P	P	P	1	2	3	4	5	6
	8	9	P	P	P	P	P	P	P	P	P	P	1	2	3	4
	5	6	8	9	P	P	P	P	P	P	P	P	P	P	P	1
	2	3	4	5	6	8	9	7	10	11	12	13	15	16	17	P

← 16 →

↑ 4 ↓

1. Each block in Modes Cr1-6 includes 2 PHA event readouts (80 bits) and one rate group (40 bits). The group read out is designated by the number in the block.
2. Each block in Mode Cr5A represents a single PHA event or a single rate group.
3. Subcommutation and Frame Counter advance are performed at Group 15 readout.
4. Motor steps one sector every 6 minutes in Modes Cr1-6, once every 3.2 minutes in Mode Cr5A.

Table 5-4 Far Encounter Mode Data Format, LECP

1	P	2	3	P	4	1	P	2	7	P	5	1	P	2	3	P	6
1	P	2	9	P	4	1	P	2	3	P	5	1	P	2	11	P	6
1	P	2	3	P	4	1	P	2	8	P	5	1	P	2	3	P	6
1	P	2	10	P	4	1	P	2	3	P	5	1	P	2	12	P	6
1	P	2	3	P	4	1	P	2	7	P	5	1	P	2	3	P	6
1	P	2	9	P	4	1	P	2	3	P	5	1	P	2	13	P	6
1	P	2	3	P	4	1	P	2	8	P	5	1	P	2	3	P	6
1	P	2	10	P	4	1	P	2	3	P	5	1	P	2	14	P	6
1	P	2	3	P	4	1	P	2	7	P	5	1	P	2	3	P	6
1	P	2	9	P	4	1	P	2	3	P	5	1	P	2	15	P	6
1	P	2	3	P	4	1	P	2	8	P	5	1	P	2	3	P	6
1	P	2	10	P	4	1	P	2	3	P	5	1	P	2	11	P	6
1	P	2	3	P	4	1	P	2	7	P	5	1	P	2	3	P	6
1	P	2	9	P	4	1	P	2	3	P	5	1	P	2	12	P	6
1	P	2	3	P	4	1	P	2	8	P	5	1	P	2	3	P	6
1	P	2	10	P	4	1	P	2	3	P	5	1	P	2	13	P	6
1	P	2	3	P	4	1	P	2	7	P	5	1	P	2	3	P	6
1	P	2	9	P	4	1	P	2	3	P	5	1	P	2	16	P	6
1	P	2	3	P	4	1	P	2	8	P	5	1	P	2	3	P	6
1	P	2	10	P	4	1	P	2	3	P	5	1	P	2	17	P	6

← 18 →

↑ 20 ↓

1. Each block marked P represents a PHA readout (40 bits)
2. Numbered blocks represent rate group readouts (40 bits each)
3. Sequence requires 24 sec at readout rate of 600 bps.
4. Subcommutation and Frame Counter advance performed at Group 15 readout.
5. Motor steps once per sequence (24 sec)

Table 5-5. LECP Rate Channel Groups  
Near Encounter Mode

Group Number	Rate Channels in Group			
1	P $\alpha$ 1	P $\alpha$ 2	P $\alpha$ 3	E $\beta$ 4
2	E $\beta$ 1	E $\beta$ 2	E $\beta$ 3	E $\gamma$ 6
3	P $\delta$ 9*	P $\delta$ 10*	P $\delta$ 11*	A $\delta$ 3*
4	E $\gamma$ 7	E $\gamma$ 8	E $\gamma$ 9	E $\beta$ 5
5	PSA3*	PSB3*	PAB12*	PAB13*
6	P $\alpha$ 4	P $\alpha$ 8	ESA0*	ESB0*
7	PSA1*	PSB1*	PSA2*	PSB2*
9	EAB10*	P $\alpha$ 5	P $\alpha$ 6	P $\alpha$ 7
15	A $\alpha$ 1	A $\alpha$ 2	Z $\delta$ 1	A $\delta$ 4
17	I $\alpha$	I $\beta$	**S5,S1,S6,S2	**S5,S3,S6,S4
18	Single Selected Rate Channel			

LEMPA	Status
-------	--------

\* Rate accumulators shared with Cruise Mode channels  
\*\* Subcommutated status bits

Table 5-6. Near Encounter Mode Data Format, LECP

1	2	3	4	5	6	1	2	3	4	7	9	1	2	3	4	15	17
1	2	3	4	5	6	1	2	3	4	7	9	1	2	3	4	15	17
1	2	3	4	5	6	1	2	3	4	7	9	1	2	3	4	15	17
1	2	3	4	5	6	1	2	3	4	7	9	1	2	3	4	15	17
1	2	3	4	5	6	1	2	3	4	7	9	1	2	3	4	15	17
1	2	3	4	5	6	1	2	3	4	7	9	1	2	3	4	15	17
1	2	3	4	5	6	1	2	3	4	7	9	1	2	3	4	15	17
1	2	3	4	5	6	1	2	3	4	7	9	1	2	3	4	15	17
18	18	18	18	18	18	18	18	18	18	18	18	18	18	18	18	18	18

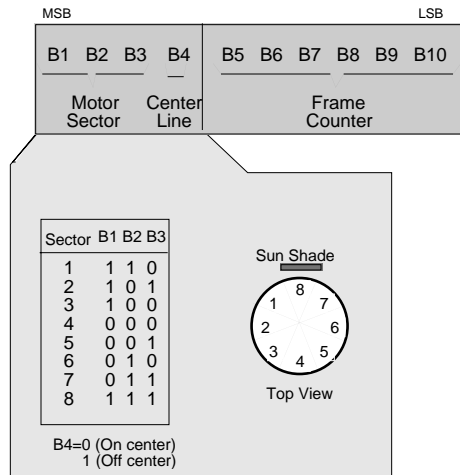
← 18 →

↑ 10 ↓

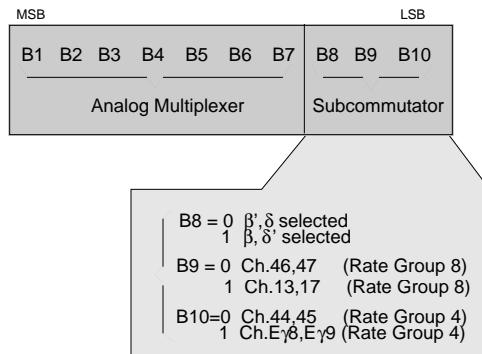
1. No PHA readout
2. Each block represents a rate group readout.
3. Sequence requires 12 sec at 600 bps.
4.  $\beta, \beta'$  and  $\delta, \delta'$  switch at the start of each group 15 readout.

Table 5-7 LECP Status Words

- S1\_\_\_ State of Command Word #1
- S2\_\_\_ State of Command Word #2
- S3\_\_\_ State of Command Word #3
- S4\_\_\_ State of Command Word #4
- S5\_\_\_ Motor Position and Frame Counter



- S6\_\_\_ Multiplexers and Subcommutator





## References

Krimigis, S. M., T. P. Armstrong, W. I. Axford, C. O. Bostrom, C. Y. Fan, G. Gloeckler, and L. J. Lanzerotti, The Low Energy Charged Particle (LECP) experiment on the Voyager spacecraft, *Space Sci. Rev.*, 21, 329, 1977.

Krimigis, S. M., J. F. Carbary, E. P. Keath, C. O. Bostrom, W. I. Axford, G. Gloeckler, L. J. Lanzerotti, and T. P. Armstrong, Characteristics of the hot plasmas in the Jovian magnetosphere: Results from the Voyager spacecraft, *J. Geophys. Res.*, 86, 8227, 1981.

Krimigis, S. M., J. F. Carbary, E. P. Keath, T. P. Armstrong, L. J. Lanzerotti, and G. Gloeckler, General characteristics of hot plasma and energetic particles in the Saturnian magnetosphere: Results from the Voyager spacecraft, *J. Geophys. Res.*, 88, 8871, 1983.

Mauk, B. H., S. M. Krimigis, E. P. Keath, A. F. Cheng, T. P. Armstrong, L. J. Lanzerotti, G. Gloeckler, and D. C. Hamilton, The hot plasma and radiation environment of the Uranian magnetosphere, *J. Geophys. Res.*, 92, 15283, 1987.

Mauk, B. H., S. A. Gary, M. Kane, E.P. Keath, S. M. Krimigis, and T. P. Armstrong, Hot plasma parameters of Jupiter's inner magnetosphere, *J. Geophys. Res.*, 101, 7685, 1996.